Universidade de Aveiro Departamento de Ciências Médicas
2017

JOANA RITA FANECA SANTOS

Fosforilação da TAU Thr231 como um potencial biomarcador da Doença de Alzheimer

TAU Thr231 phosphorylation as a potential Alzheimer's disease biomarker

Universidade de Aveiro
2017

Departamento de Ciências Médicas

JOANA RITA FANECA SANTOS

Fosforilação da Tau Thr231 como um potencial biomarcador da Doença de Alzheimer

TAU Thr231 phosphorylation as a potential Alzheimer's disease biomarker

Dissertação apresentada à Universidade de Aveiro para cumprimento dos requisitos necessários à obtenção do grau de Mestre em Biomedicina Molecular, realizada sob a orientação científica do Professor Doutor Jens Wiltfang, Professor Catedrático Convidado do Departamento de Ciências Médicas da Universidade de Aveiro e co-orientação da Professora Doutora Odete da Cruz e Silva, Professor Auxiliar c/ Agregação do Departamento de Ciências Médicas da Universidade de Aveiro

t

Esta dissertação contou com o apoio financeiro do Instituto de Biomedicina (iBiMED) - UID/BIM/04501/2013 e PTDC/DTPPIC/5587/2014 da Fundação para a Ciência e Tecnologia do Ministério da Educação e Ciência, programa COMPETE, do QREN e da União Europeia (Fundo Europeu de Desenvolvimento Regional).

Dedico esta dissertação de mestrado aos meus pais e ao meu irmão pelo incansável apoio em todas as etapas da minha vida

o júri

presidente	Professora Doutora Odete Abreu Beirão da Cruz e Silva Professora Auxiliar C/ Agregação, Universidade de Aveiro
arguente	Doutora Sónia Cristina das Neves Ferreira Investigadora de Pós Doutoramento, Centro de Neurociências e Biologia Celular - Universidade de Coimbra
orientador	Professor Doutor Jens Wiltfang Professor Catedrático Convidado, Universidade de Aveiro

agradecimentos

Um agradecimento especial ao Professor Doutor Jens Wiltfang pela oportunidade de participar neste projeto e por me ter recebido tão bem. Obrigada por permitir o meu enriquecimento científico e profissional.

À Professora Doutora Odete da Cruz e Silva pela sua orientação, apoio, dedicação e encorajamento durante a realização desta dissertação.

À Professora Doutora Ana Gabriela Henriques e à Professora Doutora Sandra Rebelo pela sua disponibilidade.

A todos os colegas do Laboratório de Neurociências e Sinalização Celular, em especial à Tânia e ao André pelo apoio científico sem o qual o sucesso deste trabalho não seria possível.

Ao iBiMED, Universidade de Aveiro (UA), pelas instalações e equipamento.
À FCT pelo financiamento do projecto PTDC/DTPPIC/5587/2014.

A todos os meus amigos, desde os de sempre aos que fui fazendo neste percurso académico, da Covilhã a Aveiro, obrigada pela vossa amizade.

Um agradecimento especial à Filipa Marques e Maria Abrantes por todo o apoio.

À minha família pelo amor, apoio e coragem que sempre me transmitiram e sem os quais este trabalho não seria possível.

E um obrigado à gente da minha terra, pela coragem e raça que me demonstraram ao se conseguirem levantar das cinzas.

palavras-chave SH-SY5Y, diferenciação, amostras clinicas, LCR, sangue, demência, ApoE, fosforilação, neuroquímico, Abeta

resumo A doença de Alzheimer (AD) é uma doença neurodegenerativa progressiva caracterizada pela presença de placas de amilóide extracelulares (placas senis) e tranças neurofibrilhares intracelulares formadas pela proteína TAU hiperfosforilada. A proteína TAU quando hiperfosforilada perde a capacidade de se ligar a microtúbulos e pode ser libertada para fluidos periféricos. Este processo leva à degradação neuronal e à morte neuronal. A fosforilação na treonina 231 tem-se demonstrado ser específica para a AD e preceder a formação de filamentos helicoidais emparelhados no cérebro humano. Para melhor perceber a função deste resíduo e a contribuição para a localização da TAU, analisámos células SH-SY5Y indiferenciadas e células diferenciadas, pela adição de ácido retinoico (RA). O tratamento com RA aumentou a expressão de TAU fosforilada na Thr231 (TAUpThr231) conforme determinado por Western blot. Explorámos ainda a fosforilação da TAU por imunocitoquímica e percebemos que em células SH-SY5Y indiferenciadas, a phosphoTAU231 estava localizada principalmente no núcleo. Em contraste, TAU e phosphoTAU231 foram redistribuídas para as dendrites e citosol das células SH-SY5Y diferenciadas pelo ácido retinoico (RA). Para avaliar o potencial deste resíduo como biomarcador; medimos TAUpThr231 em CSF por meio de um imunoensaio enzimático em sanduíche e observámos que a proporção de níveis de TAUpThr231 / TAU discriminou de forma significativa o grupo AD do grupo não-AD. Essas descobertas podem indicar que os níveis da relação TAUpThr231 / t-TAU podem ser um marcador valioso para o diagnóstico clínico de AD, independentemente da idade e do género.

keywords SH-SY5Y differentiation, clinical samples, CSF, blood, dementia, ApoE, phosphorylation, neurochemical, Abeta

abstract Alzheimer's disease (AD) is a progressive neurodegenerative disorder characterized by the presence of extracellular amyloid plaques (senile plaques) and intracellular neurofibrillary tangles formed by hyperphosphorylated TAU protein. TAU protein when hyperphosphorylated loses the ability to bind to microtubules and can be released into peripheral fluids. This process leads to neuronal degradation and neuronal death. Phosphorylation at threonine 231 has been shown to be specific for AD and to precede assembly of paired helical filaments in the human brain. In order to understand more about this residue we analysed SH-SY5Y cells undifferentiated and in differentiated cells induced by retinoic acid (RA). Treatment with RA increased expression of TAU phosphorylated at Thr231 (TAUpThr231) as determined by Western blot analysis. We further explored TAU phosphorylation by immunocytochemistry and noticed that in undifferentiated SH-SY5Y cells, TAUpThr231 was located mainly in the nucleus. In contrast, TAU and TAUpThr231 was redistributed to the neurites and in the soma of SH-SY5Y cells, which were induced to differentiate by retinoic acid (RA). In order to evaluate the potential of TAUpThr231 as a biomarker, we measured TAUpThr231 in CSF by a sandwich enzyme immunoassay and observed that the ratio of TAUpThr231/TAU levels discriminated significantly the AD group for the non-AD group. These findings indicate that TAUpThr231/t-TAU ratio levels may be a valuable marker for the clinical diagnosis of AD, irrespective of age and gender.

Index

I. List of figures

II. List of tables

III. Abbreviations

Abeta/Aβ	Beta-Amyloid peptide
ABCA7	ATP-binding cassette, subfamily A (ABC1), Member 7
AD	Alzheimer´s disease
AICD	Amyloid precursor protein intracellular domain
AMPK	5' Adenosine monophosphate-activated protein kinase
APS	Ammonium persulfate
ApoE	Apolipoprotein E
APP	Alzheimer´s amyloid precursor protein
ATP	Adenosine triphosphate
BACE	Beta-site APP-cleaving enzyme
BCA	Bicinchoninic acid
BIN1	Bridging integrator 1
BRSK	Brain-specific kinase ½
BSA	Bovine serum albumin
CaMK-II	Calcium/calmodulin-dependent protein kinase II
CD2AP	CD2- associated protein
Cdk2	Cyclin-dependent protein kinase 2
Cdk5	Cyclin-dependent protein kinase 5
CHK1	Checkpoint Kinase 1
CHK2	Checkpoint Kinase 2
CK1	Casein kinase 1
CK2	Casein kinase 2
CLU	Clusterin
CNS	Central nervous system
CR1	complement component (3b/4b) receptor 1
CSF	Cerebrospinal fluid
CT	Computarized tomography
C-terminal	Carboxyl-terminal
CTF	Carboxyl-terminal fragment
DTT	Dithiothreitol
DYRK1A	Dual-specificity tyrosine phosphorylation-regulated kinase 1A
ECL	Enhanced chemiluminescence
EDTA	Ethylenediamine tetraacetic acid
ELISA	Enzyme Linked Immuno Sorbent Assay
EOAD	Early-onset Alzheimer's Disease
EPHA1	EPH receptor A1
ERK	Extracellular signal–regulated kinases
FBS	Fetal bovine serum
FDG	Fluorodeoxyglucose
FYN	Proto-oncogene tyrosine-protein kinase
GSK3	Glycogen synthase kinase 3
HRP	Horse radish peroxidase
HSA	Human serum albumin
IB	Immunoblotting
IgG	Immunoglobulin G
IP	Ammonium persulfate

JNK	c-Jun N-terminal Kinase
LB	Loading Buffer
LGB	Lower gel buffer
LOAD	Late-onset Alzheimer's Disease
LRRK	Leucine-rich repeat kinase 2
MAP	Microtubule associated proteins
MAPK	Mitogen activated protein kinases
MAPT	Microtubule Associated Protein TAU
MARK	Microtubule-affinity regulating kinase
MBD	Microtubule-binding domain
MCI	Mild Cognitive Impairment
MET	Tyrosine kinase
MRI	Magnetic resonance imageing
MS4A6A	Membrane-spanning 4-domains, subfamily A, members 6A
MS4A4E	Membrane-spanning 4-domains, subfamily A, members 4E
MSK1	Mitogen- and stress-activated protein kinase
NFT	Neurofibrillary tangles
NMDA	N-Methyl-D-aspartic acid
NPDPK	Non - Proline directed protein kinases
N-terminal	Amino-terminal
O-GlcNac	O-linked N-acetylglucosamine
P38	p38 mitogen-activated protein kinase
P10S6K	Ribosomal protein S6 kinase beta-1
PBS	Phosphate buffered saline
PBS-T	Phosphate buffered saline – tween
PDPK	Proline directed protein kinases
PEN-2	Presenilin enhancer 2
PET	Positron emission tomography
PFA	Paraformaldehyde
PHF	Paired helical filaments
PhK	Phosphorylase kinase
PIB	Pittsburgh Compound B
PICALM	Phosphatidylinositol Binding Clathrin Assembly Protein
PIN1	Protein interacting with NIMA
PK	Protein kinase
PKA	Protein kinase A
PKB	Protein kinase B
PKC	Protein kinase C
PKN	Protein kinase N
PP	Protein phosphatase
PSEN1	Presenilin 1
PSEN2	Presenilin 2
PSK1/TAOK2	Prostate-derived sterile 20-like kinase 1 alpha/beta
PSK2/TAOK1	Prostate-derived sterile 20-like kinase 2
pTAU	Phosphorylated TAU
RIPA	Radio-Immunoprecipitation Assay
ROCK	RHO-associated kinase
RSK1/2	90 kDa ribosomal S6 kinase
RT	Room temperature
SAP	Stress-activated protein

SAPK	Stress-activated protein kinase
sAPP	Secreted APP
SDS	Sodium dodecyl sulfate
SDS-PAGE	Sodium dodecyl sulfate polyacrylamide gel electrophoresis
SE	Standard error
SEM	Standard error of the mean
Ser	Serine
SGK1	Serine/threonine-protein kinase
SH3	SRC homology
SP	Senile plaques
SRPK2	Serine/arginine-rich protein-specific kinase
SYK	Spleen tyrosine kinase
TBS	Tris Buffered Saline
TBS-T	Tris Buffered Saline – tween
Thr	Threonine
TRIS	Tris(hydroxymethyl)aminomethane
TTBK	TAU tubulin kinase
Tyr	Tyrosine (Y)
UGB	Upper gel buffer
UPS	Ubiquitin–proteasome-system

1. Introduction

1. Introduction

1.1 Alzheimer's disease (AD)

As ageing of the current population rises, the incidence of neurodegenerative diseases has continuously increased. There are approximately 47 million people with dementia worldwide and this number is estimated to rise to 131 million by 2050 (1). Amongst the neurodegenerative disorders, Alzheimer´s Disease (AD) is the most common age-related dementia, generally affecting people over 65 years old. It currently affects about 24 million people worldwide, 7–8 million in Europe, 4–5 million in the USA, and 90 000 people in Portugal (2).

Alois Alzheimer initially categorized AD in 1906 after analyzing a post-mortem sample of a 51-year-old woman with signs of paranoia, sleep and memory impairment, confusion, disorientation, hallucinations and aggressive behaviour. Alois described the disease as a deterioration of the patient's memory, communication and social and physical abilities (3–5).

1.1.1 Characterizing Alzheimer's Disease

AD is characterized by progressive and insidious dysfunction affecting various cognitive and functional domains of the central nervous system leading to neuronal cell death, vascular dysfunction, and inflammatory responses. These changes are of sufficient severity to interfere with the person's ability to perform daily activities and to be self-sufficient (6).

The clinical phenotype of AD can be divided into two main stages. The first consists of a progressive and rather isolated amnestic syndrome in relation to the early involvement of the medial temporal structures. The second is characterised by the addition and the development of cognitive symptoms in the domain of executive (conceptualisation, judgment, problem solving) and instrumental (anomia, apraxia, face or object recognition) functions and become increasingly more evident, leading to severe cognitive, functional impairment and psycho-behavioural changes, due to the increased burden and progression of neuronal lesions to the neocortical areas (6,7). All these symptoms progressively impact on the autonomy of the patient defining the dementia stage.

Patients in more advanced states become very susceptible to infections, pneumonia and decubitus ulcers. The life expectancy after diagnosis of AD is usually between 4 to 8 years, yet some patients can live as long as 20 years with the disease (8).

1.1.2 Neuropathological hallmarks of Alzheimer's Disease

AD patients' brains are normally characterized by severe neuronal loss confined to specific areas or layers of the cortex leading to cortical atrophy in the form of gyral shrinkage, widening of the sulci and enlargement of the ventricles (9).

The primary brain regions affected are the hippocampus, the neocortex and the entorhinal cortex (10). With disease progression, the neurodegeneration progresses to the temporal and parietal lobes (entorhinal cortex, hippocampal formations, parahippocampal gyrus) areas known to be critical for long-term episodic memory, and, in some patients, even to the frontal and occipital lobes (11,12).

AD hallmarks pathologies include the extracellular deposition of Aβ peptides (amyloid plaques, designated as senile plaques (SP)), intracellular accumulation of TAU protein within neurons (neurofibrillary tangles/NFTs) and dendrites (neuropil threads) (Figure 1), and neuritic plaques in brain parenchyma, inducing defects of synaptic connections (6).

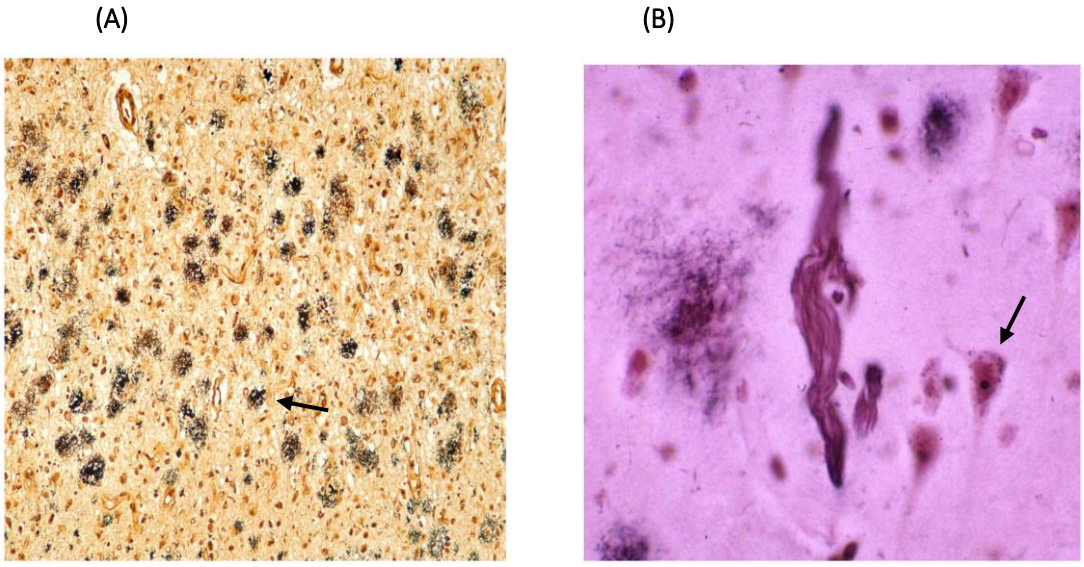

Figure 1. Neuropathological AD alterations A. Senile Plaques B. Neurofibrillary tangles (Taken from (13)*)*

Amyloid plaques are formed by the progressive accumulation of beta-amyloid (Aβ) outside the neurons (Figure 1A). Aβ deposits are morphologically diverse and result from a peptide that arises following sequential cleavage of the transmembrane amyloid precursor protein (APP) by α or β and γ secretases. The processed Aβ can accumulate extracellularly, where it aggregates into plaques (6).

APP undergoes cleavage during its transport through the axons to the synaptic terminals, where it accumulates in high concentrations. When APP is cleaved by the α-secretase, a soluble N-terminal amino fragment (sAPPα) and a C-terminal fragment (CTF) are released (Figure 2). Aβ is generated when the precursor protein is alternatively cleaved by a β-secretase in the N-terminal domain (Figure 2), releasing a soluble N-terminal fragment (sAPPβ), and then followed by γ-secretase cleavage at position 40 or 42 of the C-terminal end. The majority of Abeta peptides are 40 amino acids long (Aβ40). However, the Aβ42, although less abundant, is more prone to aggregate, being the most abundant species in the amyloid plaques (14). The physiological function of APP still remains largely undetermined, but it has been suggested to have a role in neurite outgrowth and synaptogenesis, transmembrane signal transduction, neuronal protein trafficking along the axon, cell adhesion, calcium metabolism, and several more (reviewed in (15)).

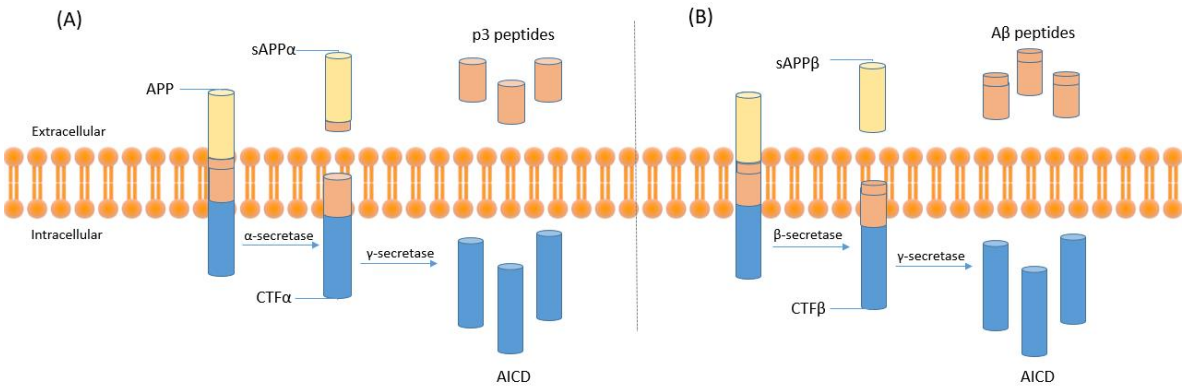

Figure 2. Proteolytic processing of APP. A. Non-amyloidogenic pathway. B. Amyloidogenic pathway. (Taken from (16)*)*

The neurotoxicity of these aggregates leads to the formation of SP which in turn lead to modifications in synaptic plasticity and neuronal integrity (17). This leads to a greater selective vulnerability of neurons which seems to contribute strongly to a cascade of events (amyloid cascade), culminating in processes of neurodegeneration and regional atrophy that appear to negatively affect other proteins, as is the case of TAU protein (18).

TAU is a microtubule-associated protein, responsible for the stabilization of microtubules. When hyperphosphorylated and misfolded, TAU is sequestered into paired helical filaments (PHF) and creates the intraneuronal aggregates know as neurofibrillary tangles (NFTs). In brains of AD patients, neurofibrillary tangles can also appear as “ghost cells” with the shape of dead neurons (Figure 1B). Consequently, the axonal cytoskeleton is disturbed, axonal transport disrupted and neuronal viability compromised (19). TAU is further discussed below.

1.1.3 Risk factors contributing to AD

AD can be early-onset/familial (EOAD) and late-onset/sporadic (LOAD). Most cases of AD occur late in life (> 65 years) as a late-onset AD. The exact causes of the late-onset AD are still imperceptible but there are a large number of risk factors that appear to contribute to the development of AD. The single most important risk factor is age, but there are also environmental, mental and lifestyle changes, female sex, low educational level, cardiovascular disease, diabetes mellitus type 2 (T2DM) and genetic risk factors (14,20).

T2DM is a risk factor based on pathology of glucose utilization. This pathology is the consequence of a disturbance of insulin-related mechanisms leading to a brain insulin resistance. Moreover, it is possible that therapeutic options utilised today for diabetes treatment may also have an effect on the risk for dementia. The contribution of T2DM and insulin-resistant brain state to cerebrovascular disturbances cannot be neglected (21).

Genetic factors account for up to 80% of the attributable risk in common AD forms. The familial AD usually develops before 65 years of age and accounts for only a small proportion (<1%) of AD cases. It is caused mainly by overproduction of Aβ caused by mutations or duplications in an APP gene or genes encoding presenilin 1 (PSEN1) or presenilin 2 (PSEN2), which are essential components of the γ-secretase complex responsible for the cleavage and release of Aβ (14).

Genetically, APP is located on chromosome 21 (21q21.2-3) and is expressed ubiquitously in all tissue types in a specific cell form. The APP gene transcribes a transmembrane protein that undergoes post-translational proteolytic processing by alpha, beta and gamma secretases. Alpha-secretase generates a soluble amyloid protein, whereas beta and gamma secretases lead to both the processing and the amyloidogenic production of Aβ. These 2 processing paths are mutually exclusive. APP mutations result in preferential processing of APP through the amyloidogenic pathway, resulting in a low concentration of alpha-sAPP in CSF which may reflect in an increased production of Aβ (22).

Down syndrome also affects the risk of AD. The additional copy of chromosome 21, where the APP gene is located, appears to increase the amount of Aβ fragments in the brain (23). Thus a direct 'load' effect is evident, whereby an extra copy of APP is associated with more Aβ production.

PSEN1 and PSEN2 are components of the γ secretase complex, responsible for the gamma-secretase-mediated proteolytic cleavage of the C-terminal transmembrane fragments of APP to produce Aβ. PSEN1 and PSEN2 mutations are associated with early-onset familial Alzheimer's disease because it can alter production of Aβ42 which leads to plaque formation more easily than with Aβ40. It has been reported that PSEN mutations may cause Alzheimer's disease through a deleterious gain of function that increases the Aβ42 amount deposited in the brain (24).

Contrary to EOAD, LOAD is considered a multifactorial disease, meaning that the individual disease risk is determined by genetic, environmental and demographic factors and the interaction between them. The strongest genetic risk factor for LOAD is the APOE gene encoding the Apolipoprotein (ApoE). ApoE is a glycoprotein for the transport of triglycerides, phospholipids, and cholesterol in cells, present in the SPs and can influence the formation of neuritic plaques. After an injury, ApoE is produced by astrocytes in the CNS to promote the protection of neurons or to repair the injured neurons. It also acts as a chaperone for Aβ by binding the peptide and altering its conformation, influencing its clearance, by transporting the peptide from the brain to the periphery, and its ability to aggregate (25).

In the APOE gene, there are three major allelic variants (-ε2, -ε3, and -ε4). These allelic variants lead to three different protein isoforms (ApoE2, ApoE3 and ApoE4) that differ in their structure, their ability to bind lipids, receptors, and Aβ, and consequently, have different transport efficiencies (25). A strong genetic association between the APOE-ε4 allele and the susceptibility of LOAD has been identified, with one APOE-ε4 allele increasing AD risk by 3-fold, and two APOE-ε4 alleles increasing AD risk by 12-fold (26,27). For APOE-ε2, compelling evidence supports a protective effect and a delaying effect on age of disease onset (28). APOE-ε3 is thought to be a neutral allele in respect to its effect upon susceptibility to AD (29).

Although APOE is the strongest genetic risk factor for LOAD, the effect of APOE-ε4 on AD susceptibility explains only a small fraction of the estimated heritability leaving most of it unexplained. In recent years, genome-wide association studies (GWAS) have identified several genes/loci, which together with APOE4, contribute to a high proportion of the genetic risk of AD. These include signals close to, or within, candidate genes such as CLU (clusterin), PICALM (phosphatidylinositol binding clathrin assembly protein), CR1 (complement component (3b/4b) receptor 1), BIN1 (bridging integrator 1), MS4A6A/MS4A4E (membrane-spanning 4-domains, subfamily A, members 6A and 4E), CD33 (CD33 molecule), CD2AP (CD2- associated protein), ABCA7 (ATP-binding cassette, subfamily A (ABC1), Member 7), EPHA1 (EPH receptor A1) and ATP5H/KCTD2 genes (review in (30–32)).

1.1.4 Diagnosing AD

Currently, the clinical diagnosis of AD is considered a two-step procedure with an initial identification of a dementia syndrome based on a detailed patients' personal and family medical history, followed by the exclusion of other possible aetiologies of dementia syndrome with physical and neurological examinations, laboratory tests and neuropsychological tests such as blood/cerebrospinal fluid (CSF) investigations for ruling out infectious, inflammatory or metabolic diseases and brain neuroimageing (CT scan or MRI) for excluding vascular diseases, infarcts and/or cerebral haemorrhages, brains tumours, hydrocephalus and similar conditions (13).

Neuroimageing techniques are also used as tools for AD diagnosis, namely computerized tomography (CT), positron emission tomography (PET) and magnetic resonance imageing (MRI). MRI enables detailed visualization and volumetric measures of the medial temporal lobe structures to detect a substantial loss of neurons, synapses, dendritic branches, and axons, as well as the expansion of the cerebrospinal fluid (CSF) spaces and alterations in the medial temporal lobe during the progression of the neurodegenerative disease (33). PET is an imageing technique that is often used with different marker compounds such as fluorodeoxyglucose (FDG) or the Pittsburgh Compound B (PIB) (Figure 3) (34). FDG-PET can measure glucose uptake in brain metabolism. In AD, a decrease in uptake of FDG-PET is an indicator of synaptic dysfunction. Pittsburgh Compound B is an amyloid radiotracer that binds specifically to beta-amyloid allowing the visualization of amyloid plaques in the cerebral cortex of patients with Alzheimer's. It has better ability to differentiate patients (with MCI, AD, and healthy controls) than FDG-PET since this technique cannot identify the abnormal protein deposits that can cause the disease (35).

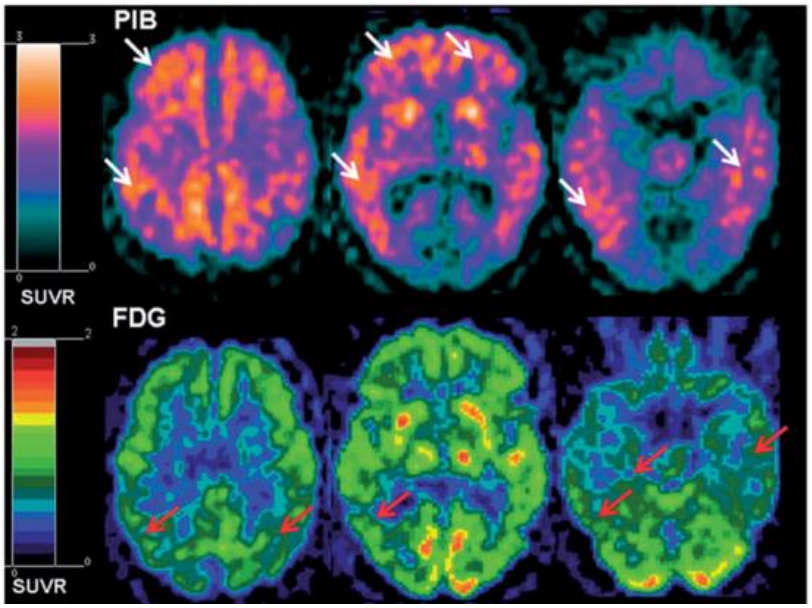

Figure 3. Amyloid deposition (upper panel, white arrows) and glucose hypometabolism (lower panel, red arrows) in an AD patient. Images from [11C]PIB-PET and [18F]FDG-PET, respectively. SUVR, standardized uptake value ratio, presented as ratios to cerebellum) (36).

This type of diagnosis can only detect the disease in a late and already symptomatic state, making it necessary to find ways to achieve an earlier diagnosis. Currently, the quantification of AD biomarkers such as Aβ and TAU, both total and phosphorylated TAU, in the CSF is the gold standard to detect early AD patients, as reviewed later in this dissertation (37).

The identification of the disease is still not perfect, and for some cases, the final confirmation arrives only with the pathological or molecular post-mortem analysis of brain tissue, where the presence of the senile plaques and neurofibrillary tangles can be confirmed (33). In the absence of such histological evidence, the clinical diagnosis of AD can only be probable and should only be made when the disease is advanced and reaches the threshold of dementia. For the diagnosis of probable AD, a dementia syndrome must be established by clinical examination, documented by mental status questionnaire, and confirmed by neuropsychological testing.

AD is a complex disease and has no cure since the treatment is significantly impaired by the lack of accessible diagnosis that can reliably and differently detect the risk or presence of the disease (38). Current therapies for AD focus on symptomatic and neuroprotective approaches to delay the disease (review in (39)). Therefore, the development of objective biomarkers that are precise indicators of the pathogenic processes of AD is extremely important to detect the preclinical stages of AD for the early diagnosis, to monitor the progression of neurodegenerative diseases, to evaluate the responses to therapies and stratify the diseases in their different subtypes.

1.2 Biomarkers of AD

The Biomarkers Working Group of the National Institutes of Health (2001) described a biomarker as "A characteristic that is objectively measured and evaluated as an indicator of normal biological processes, pathogenic processes, or pharmacologic responses to a therapeutic intervention" (40).

Ideally, an AD a diagnostic biomarker should meet a number of criteria, including being linked to fundamental features of the neuropathology, being validated in neuropathologically confirmed cases, being able to detect the disease early in its course and to distinguish it from other dementias, having a fast, simple, accurate, non-invasive and inexpensive detection, and not be influenced by symptomatic drug treatments (35).

Before an AD biomarker could be validated it should have sensitivity and specificity of over 85%, it should have prior probability (the background prevalence of the disease in the population tested) and positive predictive value over 80% (percentage of people who are positive for the biomarker and have definite the disease at autopsy) (41).

Currently, the most interesting applications of biomarkers is achieving pre-symptomatic diagnosis of neuropsychiatric disorders, which would allow early treatment strategies at a time when more than 50% of degenerating types of neurons are still available and can be rescued, providing evidence for effectiveness of therapies and differentiate certain disorder subtypes, as in the case of 'dementias' (42).

The development of objective biomarkers that are precise indicators of the pathogenic processes of AD - degeneration of neurons and their synapses, senile plaques and neurofibrillary entanglements - is extremely important to detect the preclinical stages of AD for the early diagnosis, to monitor the progression of neurodegenerative diseases, to evaluate the responses to therapies and to stratify the disease in its different subtypes (41). There is an urgent need for a simple screening procedure that can identify patients with AD in a differential, inexpensive and non-invasive manner.

Blood is the ideal fluid for biomarkers evaluation, because it can be easily collected and have circulated through all the organs, contains secreted proteins. Changes in the concentrations of biomarkers in the blood may thus reflect changes in the disease state (33). For these reasons, the identification of novel and valid biomarkers in the blood is highly desirable and can become an essential tool for diagnosing AD.

1.2.1 Neurochemical AD Biomarkers

The most recognized biomarkers for AD are found in CSF. These include changes in levels of Aβ peptides as well as hyperphosphorylated and total TAU protein (43). These particular changes are detectable in the early stages of dementia, as well as in individuals with mild cognitive impairment (MCI) who are at high risk of transitioning to AD.

The Aβ peptides (Aβ1−40/Aβ1−42) are key molecules in the pathogenesis of AD, being the main constituent of SP. The decrease in Aβ42 concentration in CSF, but not in Aβ40 concentration, is considered a reliable diagnostic biomarker of AD. There are several potential mechanisms that try to explain this decrease of Aβ42 CSF concentrations in AD. One of these possible explanations could be a hypothetical decrease in the Aβ generation. This, however, stays in disagreement with the increased of the Aβ42 in the brain tissue (42). Another mechanism might be Aβ42 increased degradation, however, this should affect not only Aβ42 but also other Aβ peptides, at least Aβ40, since it is known that both peptides are largely metabolized by the same enzymes, also it should lead to the decrease of the formation of Aβ42 deposits in the brain parenchyma, and should prevent formation of the plaques. The next potential explanation is the increased Aβ42 clearance from the brain tissue to the blood across the blood-brain barrier. This would lead to the decreased amount of the Aβ42 molecules in the brain parenchyma and correspondingly less Aβ42 molecules could enter the CSF, but it was reported a decreased Aβ42 concentrations and/or Aβ42/40 ratios in the blood of AD patients or subjects at AD risk (44). Finally, there is a very interesting, hypothesis that the CSF concentrations of Aβ42 in AD patients only seems decreased, because the accumulation of Aβ42 monomers into soluble oligomers leads to masking of the epitopes for the antibodies used in the ligand-based analytical methods. Indeed, increased concentrations of Aβ oligomers were reported, in the CSF of AD patients (44).

Irrespective of the cause of decreased Aβ42 concentration in CSF, sensitivity and specificity of Aβ42 alone to distinguish AD from elderly controls were 78% and 81%, respectively (45).

Better diagnostic performance of the Aβ42/40 ratio compared to the Aβ42 concentration might then be explained by the assumption that the subjects with either extraordinary low or extraordinary high concentrations of total Aβ peptides in the CSF characterise also with the respectively low or high Aβ42 (46). In such a case, a normalisation of the Aβ42 concentration by the application of the Aβ42/40 ratio, instead of the Aβ42 alone, improves the interpretation of the biomarkers. This decrease in Aβ42/Aβ40ratios in CSF most likely reflects the precipitation of Aβ42 into SPs in the cerebral parenchyma (35).

The microtubule-associated protein TAU is the major component of intraneuronal NFTs observed in AD, frontotemporal dementia and in a group of more than 20 other Tauopathies. TAU protein (described in detail below) undergoes chemical changes that make it hyperphosphorylated, converting TAU from a normal functional protein to a neurotoxic protein, giving rise to neurofibrillary tangles (35).

In AD, TAU concentrations tend to increase and although this is not a specific biomarker for AD, it is clinically associated with the severity of the disease. TAU is generally thought of as an intracellular protein which is released only upon axonal degradation and neuronal death, into the extracellular space. Thus TAU can then be transported to the peripheral fluids, making it detectable in peripheral bodily fluids such as CSF, plasma and/or serum (33). Abnormal concentrations of phosphorylated TAU protein (pTAU) in CSF have been proposed as a biomarker of AD since many neurodegenerative diseases can be distinguished by the set of TAU isoforms that accumulate in neurons (47). CSF TAU provides a useful marker of TAU pathology and can be used to monitor the efficacy of disease-modifying therapies (48).

Currently, no biomarker meets the criteria of an ideal biomarker for AD, as the CSF is only assessable by lumbar puncture, which is still considered a relatively invasive practice that may cause discomfort to the patient and present some side effects. Nevertheless, CSF alterations are, at least currently, the first that can be observed in the disease process. The combination of three CSF biomarkers, namely TAU, pTAU181 and Aβ42 are still the best available markers, with a sensitivity of 68% (95% CI 45–86%) and a specificity of 97% (95% CI 83–100%) to detect incipient AD among patients fulfiling the criteria for MCI (49,50).

An algorithm has been proposed to interpret the levels of these biomarkers, called the Erlangen Score Algorithm (Figure 4). In brief, depending on the concentrations of the biomarkers, the numeric score is given, and the final sum (in the range 0–4 points) defines the categorisation of a given patient into one of the groups with different probability of AD pathology, which is eventually presented to the physician on the CSF integrated report (36,51).

	Aβ Normal (0)	Aβ in Border Zone (+1)	Aβ Pathologic (+2)
TAU/pTAU Normal (0)	0	1	2
TAU/pTAU in Border Zone (+1)	1	2	3
TAU/pTAU Pathologic (+2)	2	3	4

Figure 4. Erlanger Score. Erlangen Score is the sum of the scores for Aβ biomarkers (0, normal; 1, borderline pathological; 2, pathological) and TAU/pTAU biomarkers (0, normal; 1, borderline pathological; 2, pathological), always in relation to a given laboratory's cut-offs. Depending on the total score, NDD is interpreted as: 0, neurochemically normal; 1, AD neurochemically improbable; 2–3, AD neurochemically possible; 4, AD neurochemically probable. (Taken from (36)*)*

If the results of Aβ and TAU/pTAU are pathological, the overall result is interpreted as a neurochemically probable AD.

1.3 Microtubule-Associated Protein TAU

The microtubule-associated protein TAU is quite abundant in the CNS's neurons, especially in the distal termination of the axon and is important for the neuronal morphogenesis, brain development, and is involved in the regulation of microtubule dynamics (52). TAU changes such as abnormal cleavage and phosphorylation are a major component of intraneuronal aggregates observed in Alzheimer's disease and other Tauopathies. The excessive phosphorylation of TAU detaches the protein from the microtubule causing microtubule destabilization (53). This alteration of microtubule equilibrium may result in axonal transport disturbances.

TAU proteins are part of the microtubule-associated proteins (MAP) family and they are mainly detected in the axons of neurons, in the cytosol, in association with plasma membrane components and also in the nuclei of neurons. Non-neuronal cells like glial cells can also have traces of TAU, but mainly in pathological conditions (54).

1.3.1 Gene and Protein Structure

The human MAPT gene (codes for TAU protein) is located on the long arm of chromosome 17, at band position 17q21. The TAU primary transcript comprises 16 exons and codes a total of six different mRNA species that are translated in six different isoforms of TAU with a range from 352 to 441 amino acids, expressed in the adult human CNS (55) via alternative splicing (54).

Brain TAU proteins have two domains: the projection domain and the microtubule-binding domain (Figure 5). The projection domain in the N-terminal region can be subdivided into an acidic region, which is encoded by exons 1–5 and a proline-rich region encoded by exon 7 and the first half of exon 9. This domain is responsible for the interactions with proteins associated with the neural plasma membrane and cytoplasmatic organelles and determines spacings between axonal microtubules. The microtubule-binding domain is subdivided into a region responsible for TAU binding with microtubules which are encoded by exons 9–12 and contains four repeat domains R1, R2, R3, and R4 also called MBDs (microtubule-binding domains) and a short C-terminal region which is encoded by exon 13 (56). As its name suggests, this domain is responsible for the binding of TAU to microtubules, especially through the repeat domains which are also responsible for promoting microtubule polymerization and stabilization (54).

In the human brain, TAU proteins are a family of six isoforms, which range from 352 to 441 amino acids (55), all of which are phosphorylated by glycogen synthase kinase 3 (GSK 3) (57). They differ from each other by the presence of either three (3R) or four (4R) conservative tubulin binding

repeats of 31–32 amino acids in the carboxy-terminal (C-terminal) part of the molecule and the absence (0N) or presence of one (1N), or two (2N) inserts (29 or 58 amino acids) at the amino-terminal (N-terminal) part (55). Thus, the longest isoforms in the CNS has four repeats and two inserts (441 residues), and the shortest isoform has three repeats and no inserts (352 residues) (Figure 5).

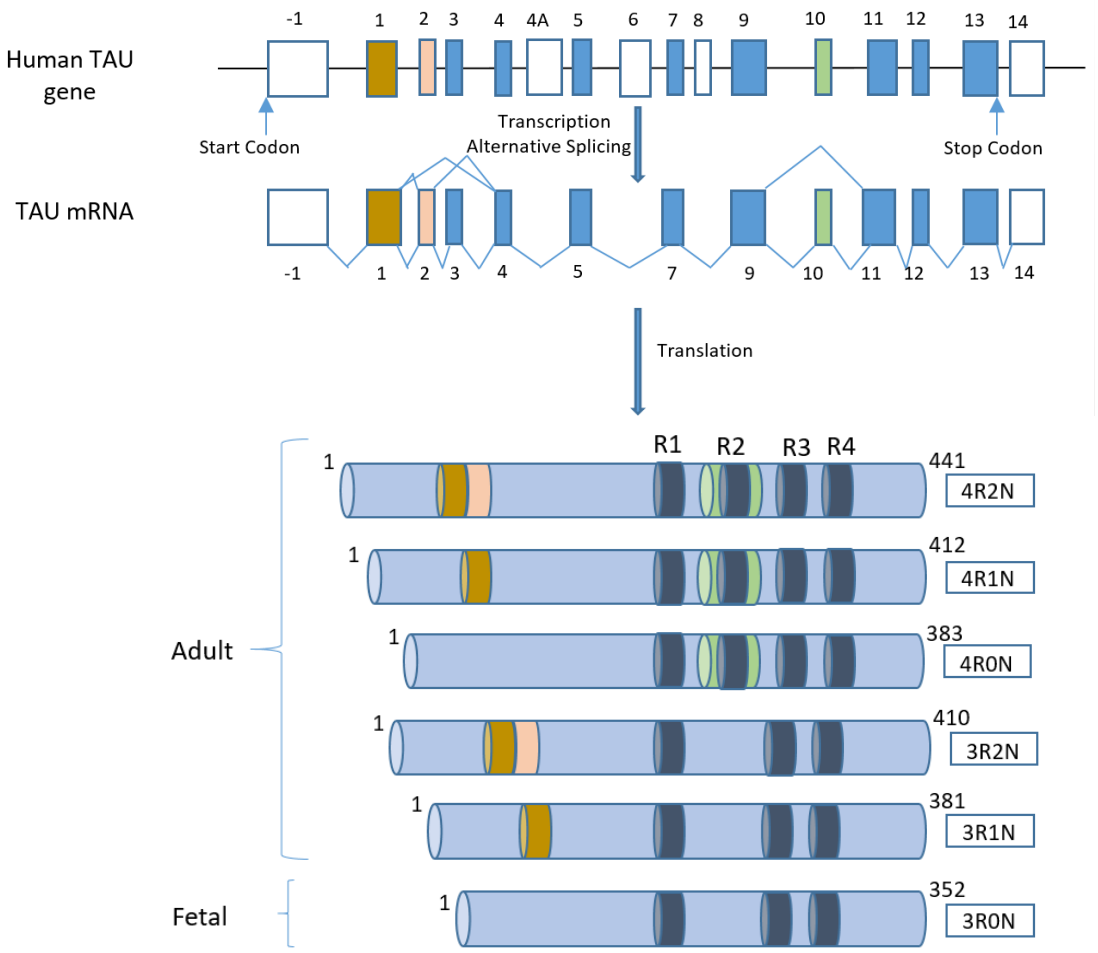

Figure 5. Schematic representation of the human TAU gene, mRNA and different protein isoforms. The human TAU gene is located over 100kb on the long arm of chromosome 17 at position 17q21. It contains 16 exons; exon -1 is a part of the promoter. The TAU primary transcript contains 13 exons since exons 4A, 6 and 8 are not transcribed in human. Exons -1 and 14 are transcribed but not translated. Exons 1, 4, 5, 7, 9, 11, 12, 13 are constitutive, and exons 2, 3 and 10 are alternatively spliced, giving rise to six different mRNAs, translated in six different TAU isoforms. These isoforms differ by the absence or presence of one or two 29 amino acids inserts encoded by exon 2 and 3 in the amino-terminal part, in combination with either three (R1, R3 and R4) or four (R1, R2, R3 and R4) repeat-regions in the carboxyl-terminal part. (taken from (54))

The length of the projection domain further increases the diversity of TAU isoforms, by the number of repeat motifs, depending on exon alternative splicing and by various post-translational modifications. Each of these isoforms is likely to have particular physiological roles since they are differentially expressed during development.

1.3.2 TAU Function in the CNS

The physiological role of TAU is still not fully understood. Some studies suggest that one of the major biological functions of TAU is to promote microtubule assembly and stability in axons, due to their C-terminal microtubule-binding domain, which is essential for axonal transport, and might be involved in the creation and maintenance of neuronal polarity. The N-terminal region jointly with the proline-rich domain creates projections from the microtubules' surface to adjacent microtubules, binding the neural plasma membrane components. This suggests that TAU functions as a linker protein between both, therefore, contributing to the parallel ordered organization of microtubules in axons (58). TAU proteins are also involved in promoting microtubule nucleation, growth and bundling, and it is hypothesized that phosphorylation of the TAU molecule is an important factor in regulating TAU-microtubule interaction (reviewed in (59)).

1.3.3 Post-translational modifications of TAU protein

TAU protein, like many other proteins that are implicated in human disease, undergoes various post-translational modifications, including phosphorylation, glycosylation, ubiquitination, glycation, truncation, nitration, among others. An increased amount of the modified TAU has been found in a large number of neurodegenerative disorders (60).

Glycosylation is an enzymatic process through which a covalent attachment of oligosaccharides to the side chain of polypeptides is formed. There are two types of glycosylation, N- and O-glycosylation, according to the nature of glycosidic bonds. N- Glycosylation results from the attachment of sugars are linked to the amide group of the asparagine, while O- glycosylation is characterized by the addition of an O-linked N-acetylglucosamine (O-GlcNac) residue to the hydroxyl group of serine or threonine near the proline residue (56). In AD brains, the level of N-Glycosylation is enhanced and the level of O-GlcNac is decreased. Furthermore, it is believed that O-glycosylation may protect TAU from hyperphosphorylation and prevent, consequently, NFT formation (60).

Glycation refers to a non-enzymatic linkage of a reducing sugar to the amino side chain of a polypeptide. In TAU isolated from PHF glycation can be present whereas no glycan has been detected

in normal TAU. Glycation is involved in the early disease process and appears to enhance the formation of PHF and its aggregation into more complex aggregates. Moreover, it has been found that the glycated TAU can disturb neuronal function by generating oxygen free radicals (61).

Ubiquitination is the specific binding of a 76-amino acid protein, ubiquitin, on proteins to signal for their degradation in an ATP-dependent manner by the UPS (ubiquitin–proteasome-system). In non-pathological conditions, TAU exists as an unfolded protein and it can be ubiquitinated and proteolytically processed by UPS. In AD, high levels of ubiquitinated TAU can be found in aberrant aggregates or in some types of paired helical filaments (61).

TAU truncation consists of the cleavage of TAU that occurs at the glutamic acid residue 391. These truncated TAU proteins are conformationally different enhancing their capacity to form aggregates and contributing to the execution of neuronal apoptosis (61).

Nitration is the addition of nitrogen dioxide to a tyrosine of an organic molecule and it has been suggested to be increased in AD brains (56). TAU nitration is involved in TAU aggregation and may represent oxidative damage of the brain as the accumulation of oxidants may be important for the nitration of TAU in AD brains (60).

1.3.3.1 *TAU phosphorylation*

Protein phosphorylation is the most common TAU post-translational modification in which a covalently bound phosphate group is added to an amino acid residue by a protein kinase. Even though TAU phosphorylation plays a key role in regulating the physiological functions of TAU at different neuronal locations, it has been reported that phosphorylation at the microtubule-binding domain (Figure 6), at the KXGS motifs, reduces its affinity for microtubules which results in the destabilization of the cytoskeleton of neurons (62).

There is a total of 85 potential phosphorylation sites at three types of amino acids: serine (S), threonine (T) and tyrosine (Y), distributed along the TAU protein. The majority of these are located in the proline-rich domain of TAU, bordering the microtubule-binding domain (Figure 6). Approximately 45 of these 85 phosphorylation sites have been found in AD brain (62,63)

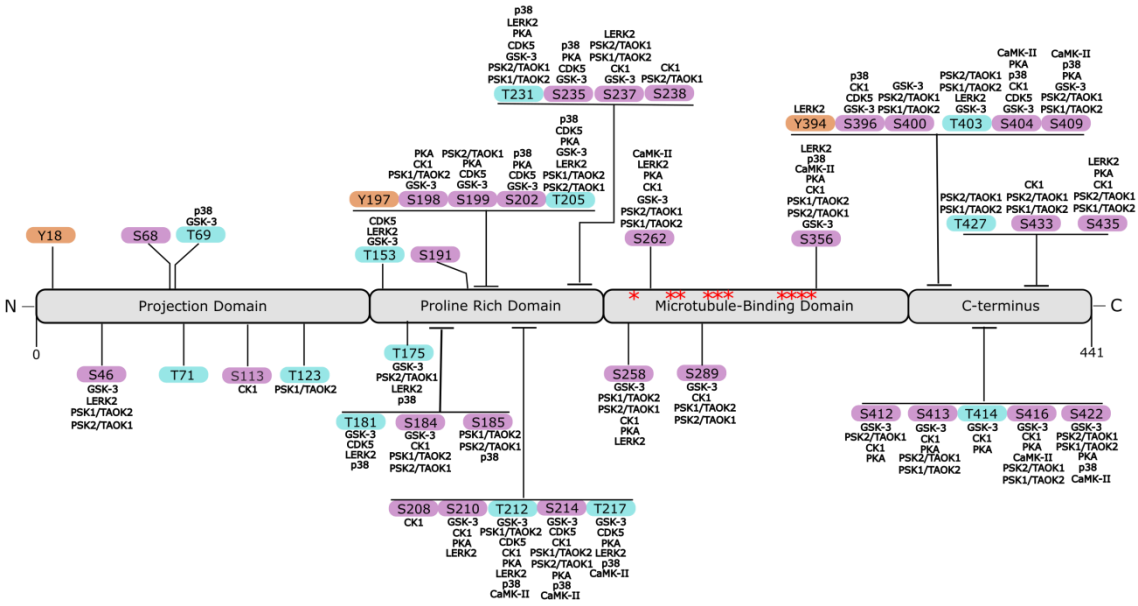

*Figure 6. TAU phosphorylation sites identified in brains of AD patients. Diagrammatic representation of the most common TAU residues (Y in orange; S in purple and T in blue) shown to be phosphorylated in the AD brain. The kinases responsible for the respective phosphorylations are also indicated (when the information was available). The KXGS motifs are indicated *259-QIGS-262, **290-QCGS-293, ***321- QCGE-324, and ****353-QIGS-356. (taken from (64))*

For instance, phosphorylation at residues Ser262 (65), Ser356 and Thr231 (66) can dramatically reduce the ability of TAU to bind to microtubules, triggering its detachment (67).

The normal level of TAU phosphorylation is a result of dynamic regulation of TAU kinases and TAU phosphatases. More than 20 protein kinases in total can phosphorylate TAU proteins (68). Most of the kinases involved in TAU phosphorylation are part of the proline-directed protein kinases (PDPK), which include mitogen-activated protein kinase (MAPK), glycogen-synthase kinase-3β (GSK-3β), TAU-tubulin kinase, cyclin-dependent kinases including CDC2 and CDK5 and stress-activated kinases (SAP kinases). Another group named non-PDPK or NPDPK comprises microtubule-affinity regulating kinase (MARK), Ca2+/calmodulin-dependent protein kinase II (CaMPKII), cyclic-AMP-dependent kinase (PKA), casein kinase II and protein kinase C (PKC) (69). Among these kinases, glycogen synthase kinase-3β (GSK-3β), an isoform of GSK-3, is among the most implicated in the abnormal hyperphosphorylation of TAU in AD brains (70) and has been associated with PHF-TAU formation, neurite retraction, and neuronal death as well as a decline in cognitive performance.

Table 1. Phosphorylation sites of TAU in the Alzheimer's Disease and the site-specificity of kinases (64,71) *N.D., Not Defined.*

Human TAU residues	Kinases
Y18	FYN; SYK
S46	GSK-3β; CK1; MAPK; ERK1/2; p38; SAPK2; SAPK3
S68	N.D
T69	GSK-3; ERK; p38
T71	AMPK
S113	CK1
T123	CHK1; PSK1/TAOK2
T153	GSK-3; CDK5; ERK; SAPK1γ; SAPK2; SAPK3; SAPK4; LRRK2
T175	GSK-3β; JNK; ERK2; p38; SAPK1 γ; SAPK2; SAPK3; LRRK2; PSK2/TAOK1
T181	GSK-3β; CDK5; JNK1; JNK2; JNK3; ERK2; p38; DYRK1A; SAPK1 γ; SAPK2; SAPK3; SAPK4; LRRK2
S184	GSK-3β; CK1; SAPK2; SAPK3; PSK1/TAOK2; PSK2/TAOK1
S185	p38; PSK1/TAOK2; PSK2/TAOK1
S191	CHK1; PSK1/TAOK2; PSK2/TAOK1
Y197	MET
S198	GSK-3β; PKA; CK1; TTBK1; PSK1/TAOK2
S199	GSK-3; PKA; CDK5; CK2; MAPK; JNK1; JNK2; JNK3; ERK2; TTBK1 DYRK1A; SAPK4;
S202	GSK-3; PKA; CDK5; MAPK; JNK1; JNK2; JNK3; ERK2; p38; TTBK1; DYRK1A; SAPK1 γ; SAPK2; SAPK3; SAPK4
T205	GSK-3β; PKA; CDK5; JNK1; JNK2; JNK3; ERK2; p38; DYRK1A; SAPK1γ; SAPK2; SAPK3; SAPK4; LRRK2; PSK1/TAOK2; PSK2/TAOK1
S208	CK1δ; CHK1; TTBK1; TTBK2; AMPK
S210	GSK-3; PKA; CK1; LRRK2
T212	GSK-3; PKA; CaMK-II; CDK5; CK1; JNK1; JNK2; JNK3; ERK2; p38; DYRK1A; SAPK1γ; SAPK2; SAPK3; SAPK4; LRRK2; p70S6K; PSK1/TAOK2
S214	GSK-3β; PKA; PKB; PKC; PKN; CaMK-II; CDK2; CDK5; CK1; CHK1; CHK2; p38; SAPK1γ; SAPK2; SAPK3; SAPK4; AMPK; MSK1; p70S6K; PSK1/TAOK2; PSK2/TAOK1; RSK1/2; SGK1; SRPK2
T217	GSK-3β; PKA; CaMK-II; CDK5; JNK1; JNK2; JNK3; ERK2; p38; DYRK1A; SAPK4; LRRK2
T231	GSK-3; PKA; CDK5; JNK; ERK2; p38; DYRK1A; SAPK1γ; SAPK3; SAPK4; AMPK; LRRK2; PSK1/TAOK2; PSK2/TAOK1
S235	GSK-3; PKA; CDK5; MAPK; JNK2; ERK2; p38; SAPK1γ; SAPK2; SAPK3; SAPK4; PhK; AMPK
S237	GSK-3; CK1; PhK; LRRK2; PSK1/TAOK2; PSK2/TAOK1 CK1; PSK2/TAOK1
S238	CK1; PSK2/TAOK1
S258	GSK-3β; PKA; PKC; PKN; CK1δ; CHK1; AMPK; LRRK2; PSK1/TAOK2; PSK2/TAOK1
S262	GSK-3; PKA; PKC; CaMK-II; CK1δ; CHK1; CHK2; MARK; PhK; AMPK; BRSK; LRRK2; MSK1; p70S6K; PSK1/TAOK2; PSK2/TAOK1; ROCK
S289	GSK-3β; CK1δ; CHK1; CHK2; AMPK; PSK1/TAOK2; PSK2/TAOK1
S356	GSK-3; PKA; CaMK-II; CK1δ; JNK; MARK; ERK; CHK1; p38; SAPK1γ; SAPK2; SAPK3; SAPK4; PhK; AMPK; LRRK2; PSK1/TAOK2; PSK2/TAOK1
Y394	c-Abl; LRRK2
S396	GSK-3; CDK5; CK1; CK2; MAPK; JNK1; JNK2; JNK3; ERK2; p38; DYRK1A; SAPK1γ; SAPK2; SAPK3; SAPK4

Human TAU residues	Kinases
S400	GSK-3β; CK2; CHK1; DYRK1A; AMPK; PSK1/TAOK2; PSK2/TAOK1
T403	GSK-3β; CHK2; AMPK; LRRK2; PSK1/TAOK2; PSK2/TAOK1
S404	GSK-3; PKA; CaMK-II; CDK5; CK1; CK2; MAPK; JNK1; JNK2; JNK3; ERK2; p38; DYRK1A; SAPK4
S409	GSK-3β; PKA; CaMK-II; CHK1; CHK2; p38; SAPK3; SAPK4; PSK1/TAOK2; PSK2/TAOK1; ROCK
S412	GSK-3; PKA; CK1; CK2; PSK2/TAOK1
S413	GSK-3β; PKA; CK1; CK2; PSK1/TAOK2; PSK2/TAOK1
T414	GSK-3β; PKA; CK1δ; CK2; CHK1; PSK1/TAOK2; PSK2/TAOK1
S416	GSK-3; PKA; CaMK-II; CK1; CK2**; PSK1/TAOK2; PSK2/TAOK1
S422	GSK-3β; PKA; CaMK-II; MAPK; JNK1; JNK2; JNK3; ERK2; p38; TTBK1; DYRK1A; SAPK4;
T427	PSK1/TAOK2; PSK2/TAOK1
S433	CK1δ; CHK2; PSK1/TAOK2; PSK2/TAOK1
S435	PKA; CK1δ; CHK2; LRRK2; PSK1/TAOK2; PSK2/TAOK1 S

Regarding protein phosphatases (PP), there are four major PPs associated with TAU phosphorylation, including PP1, PP2A, PP2B (calcineurin) and PP5 (60,72). It has been found that PP2A is by far the most important and major TAU phosphatase, as it has been demonstrated to be the most effective in dephosphorylating hyperphosphorylated TAU isolated from AD brains (73).

1.3.4. Physiological and Pathological role of TAU phosphorylation

Phosphorylation can modulate the properties of TAU proteins and affect its cellular distribution in neurons, which regulates the different roles of TAU protein both in physiological and pathological conditions (54). The phosphorylation status of TAU is considered to change during development, with a relatively high degree of phosphorylation during the foetal phase followed by a steady decrease with age, possibly as a result of phosphatase activation (74).

As mentioned above, in normal conditions, TAU phosphorylation at specific sites controls a variety of processes, but when in a hyperphosphorylated state, it affects microtubule assembly and polymerization (65). As the affinity to microtubules decreases other cellular processes like axonal transport are affected (75).

TAU is present preferentially in axons, but it can appear in several cell compartments. Depending on its location the levels of TAU phosphorylation may vary, thus contributing to TAU trafficking and cell sorting (nuclear, axonal or somatodendritic) (76). The regulation of neurite outgrowth and neuronal polarization can also be controlled by phosphorylation (77). It is also noticeable that TAU phosphorylation might be developmentally regulated since it is heavily phosphorylated in foetal tissues and tends to decrease with age due to phosphatases activation (74).

Under pathological conditions, TAU is delocalized from the axons to the somatodendritic compartment of neurons, where it tends to aggregate in a hyperphosphorylated state into tangles of paired helical filaments (PHF) and straight filaments forming neurofibrillary tangles. Hyperphosphorylation is defined as a high level of phosphorylation on epitopes localized at the C-terminus and half-N-terminus of the TAU protein, outside the microtubule-binding domain. This abnormal phosphorylation is an early event of neurodegeneration and it becomes more severe with the development of the disease, affecting its physiological role (78).

In the AD brain, TAU is approximately three to four times more phosphorylated than the normal adult brain TAU (79). The aggregation of this hyperphosphorylated TAU may block the intracellular trafficking of the neurotrophins and other functional proteins, and contribute to a decline or even loss of axonal transport in the neurons (80).

Hyperphosphorylated TAU may also block intracellular trafficking in the neurons, affect cell morphology and cell growth, and promote cell cycle reentry. These changes may eventually lead to neuronal death (81).

1.3.5. TAU phosphorylation as a Predictive AD Biomarker

TAU hyperphosphorylation appear to be useful as diagnostic markers, given the correlation with relatively early events in AD development, forming the pre-tangle PHF and mature NFTs.

During this preclinical period, there is a gradual loss of axons and neurons, and the first symptoms start to appear (82). At this stage, patients do not fulfil the criteria for dementia and may be diagnosed with Mild Cognitive Impairment (MCI). People with MCI have the early neuropathology of dementia, particularly Alzheimer's disease, but do not meet the clinical criteria. These individuals are more likely to develop clinical AD at a much higher rate than normal elderly people (approximately 15% each year) (83,84). For this reason, MCI has been considered as an early stage of Alzheimer's disease and other forms of dementia, being, in some cases, the transition phase between healthy cognitive ageing and dementia (Figure 7). However, some individuals with MCI seem to remain stable or even return to normal cognition over time (85).

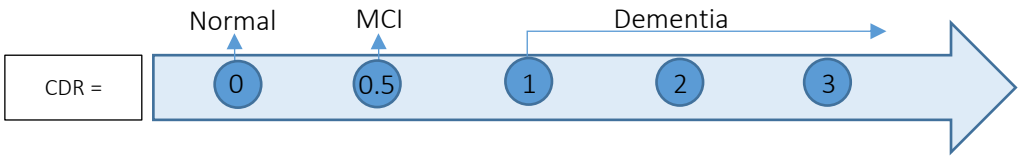

Figure 7. The spectrum of cognitive impairment (CDR - Clinical Dementia Rating scale); Adapted from (86)

It was reported that pTAU levels are increased in MCI converters (87) and that the specificity of pTAU to differentiate from other dementias is higher than that for total TAU reaching more than 80%. CSF levels of phosphorylated TAU seem to reflect both the phosphorylation state of TAU and the formation of neurofibrillary tangles in the brain.

The most studied phospho-epitopes in CSF are TAUpThr181 and TAUpThr231, which are the most reliable predictors of the decline from MCI to AD.

Although both forms show similar sensitivities and specificities for AD, TAUpThr181 is more commonly used than TAUpThr231 (88,89). High CSF TAUpThr181 has also been associated with a fast progression from MCI to AD (90) and with a rapid cognitive decline in AD (91). The majority of studies in patients with AD evaluated the levels of TAUpThr181, although the levels of TAUpThr231 have been reported to correlate better with post-mortem tangle load than do pTAU181 levels (87,92). Also, TAUpThr231 appears early in AD while TAUpThr181 occurs later (87,93).

Phosphorylation at threonine 231 has been shown to be specific for AD. Thr231 is present in pre-tangles and precedes tau oligomerization and the assembly of paired helical filaments in the human brain. The TAU Thr231 residue is localized in the projection domain of TAU protein thus

decreasing the interconnection between microtubules and other cytoskeletal components, such as actin (93). Thr231-phosphorylated TAU undergoes conformational changes that reduce the affinity of the protein for microtubules and it promotes the phosphorylation of other TAU residues (Ser199, Ser396, Ser400 and Ser404), causing TAU hyperphosphorylation and loss of function.

Buerger et al, while analysing frontal cortex homogenates and CSF samples of AD patients found significant correlations between CSF TAUpThr231 concentrations and scores of NFTs in all neocortical regions studied, indicating that CSF TAUpThr231 may serve as a surrogate biomarker of neurofibrillary pathology in Alzheimer's (94). Several other studies have shown TAUpThr231 levels to be elevated in AD compared with control subjects (95). It has also been shown to help to differentiate AD from other closely associated diseases, such as frontotemporal dementia, vascular dementia and dementia with Lewy Bodies (88).

2. Objectives of the study

2. Objectives

Alzheimer Disease (AD) is a severe age-associated disease affecting millions of people worldwide (2). The identification of the disease has some limitations, and in some cases, the final confirmation arrives only after the patient's death (33). Currently, AD diagnosis is based on a combination of several medical tools and can only detect the disease in a late and already symptomatic state.

The development of differential biomarkers that are precise indicators of the pathogenic processes of AD is extremely important to detect the preclinical stages of AD, permitting early diagnosis, to monitor the progression of neurodegenerative diseases, to evaluate the responses to therapies and stratify the diseases in their different subtypes (41). There is an urgent need for a simple screening procedure that can identify AD patients in a differentiated, inexpensive and non-invasive manner. Blood would be the ideal fluid to access biomarkers because it circulates through all the organs, but other peripheral fluids such as CSF also contain secreted proteins and may reflect changes in the state of the disease (33).

The microtubule-associated TAU protein is the major component of intraneuronal NFTs, a hallmark of AD. TAU is released only upon axonal degradation and neuronal death, making it detectable in peripheral bodily fluids (47). Phosphorylation at threonine 231 has been shown to be specific for AD and to precede assembly of paired helical filaments in the human brain.
Thus the specific aims of this dissertation are to:

- Determine the function Thr231 phosphorylation and its contribution to TAU localization in SH-SY5Y neuroblastoma cells
- To identify TAUpThr231 in CSF and blood
- To explore the potential of pTAU231 levels in the CSF as a biomarker

3. Materials and methods

3. Materials and methods

3.1. Antibodies

The following primary antibodies were used: mouse monoclonal anti-TAU antibody (Millipore, clone TAU-5, cat. # MAB361) to detect all phosphorylated and non-phosphorylated isoforms of TAU; rabbit monoclonal anti-TAU TAUpThr231 (Invitrogen/Life Technologies, clone 1H6L6, cat. # 701056), which specifically recognizes phosphorylated TAU at Thr231; Anti-Microtubule Associated Protein 2 Mouse mAb (Calbiochem, cat. #442695); Mouse Anti β-Tubulin (Invitrogen, cat. #32-2600); pTAU (Ser262), rabbit polyclonal antibody (Santa Cruz Biotechnology, cat. #sc-101813); Anti-TAU (phosphor S396) antibody (abcam, cat. #ab109390); rabbit Anti-Actin Polyclonal Antibody (Stressgen Bioreagents, cat. #CSA-400).

Table 2. Summary of the antibodies used to detect target proteins and specific dilutions used for the different assays. The specific dilutions used for the different assays are also indicated. IB: Immunoblotting; IP: immunoprecipitation; IF: immunofluorescence

Antibody	Target Protein	Reactivity	Dilution	Expected bands site (kDa)
Phospho TAU pThr 231 (Thermo)	pTAU at Thr 231	Rabbit	IB dilution: 1:250 IF dillution: 1:500	≃55
TAU-5 (Millipore)	total TAU	Mouse	IB dilution: 1:500 IF dilution: 1:200 IP dilution: 1:100	46-68
MAP2 (Calbiochem)	MAP2	Mouse	IB dilution: 1:2000 IF dilution: 1:1000	≃70
β-Tubulin (Invitrogen)	β-Tubulin	Mouse	IB dillution: 1:2000	≃50
pTAU Ser262 (Santa Cruz)	pTAU at Ser 262	Rabbit	IB dillution: 1:500	46-68
pTAU Ser396 (abcam)	pTAU at Ser 396	Rabbit	IB dillution: 1:5000	79
Anti-Actin (Stressgen)	total Actin	Rabbit	IB dillution: 1:1000	≃43

Horseradish peroxidase-conjugated anti-mouse (1:5000) and anti-rabbit (1:5000) IgGs were used as secondary antibodies (Amersham Pharmacia) for immunoblotting. For immunocytochemistry Texas Red-X goat anti-rabbit IgG (H+L) (Molecular Probes) and Alexa Fluor 488 goat anti-mouse IgG (H+L) (Life Technologies) was used as secondary antibodies (Table 2).

3.2. Cell Culture

3.2.1. Culture, growth and maintenance of SH-SY5Y cell line

In neurosciences, the use of mammalian neurons derived from embryonic the CNS tissue is very limited mainly because once these cells are terminally differentiated into mature neurons, they can no longer be propagated. To overcome this limitation transformed neuron-like cell lines are commonly used. Among them, there is a very popular and well characterized one, the SH-SY5Y neuroblastoma cell line (ATCC® CRL-2266™).(96)

The SH-SY5Y cell line was originally derived from a metastatic bone tumour biopsy, and a subline of the parental line SK-N-SH, which were subcloned three times: first to SH-SY, them to SH-SY5, and finally to SH-SY5Y.(96)

In order to archive the objectives proposed for the present study, SH-SY5Y neuroblastoma cell line was chosen for the reasons described above, and because this cell line is a human cell line that can be easily differentiated into a more mature neuronal-like phenotype.

Human SH-SY5Y neuroblastoma cells (ATCC® CRL-2266™) were grown and maintained in Minimal Essential Medium (MEM)/F12 (1:1) medium supplemented with 10% fetal bovine serum (FBS), 0.5 mM L-glutamine, 100 U/mL penicillin and 100 mg/mL streptomycin. Cultures were maintained in a humidified chamber at 37°C under 5% CO2 (96). Cells were subcultured whenever 80-90% confluence was reached. The procedures are in routine use in the laboratory.

3.2.2. Cell Differentiation

Differentiation of SH-SY5Y cells is relatively easy to achieve by manipulation of the culture medium. There are many reagents\compounds that can be added to culture medium in order to differentiate SH-SY5Y cells, but Retinoic Acid (RA) is the most commonly used (96–98).

Cells were allowed to adapt for 24 hrs (day -1) and were then subjected to differentiation. Differentiation of SH-SY5Y cells was achieved by adding all-trans-retinoic acid (RA) to the culture medium, at a concentration of 10 µM and FBS at 1%. This culture medium was replaced every 48 hours until the time of 5 days was reached.

3.2.3. Aβ Treatment

Aβ42 peptide (GenicBio Synthetic Peptide cat. #A-42-T-1)) was reconstituted in sterilized H_2O miliQ (1mM stock) and aggregated in phosphate-buffered saline (PBS, pH 7.4), for 48 h at 37°C (100 µM aggregated stock). In order to mimic AD, the cells were exposed to crescent concentrations (0, 2, 10 and 20 µM) of aggregated Aβ with the corresponding medium serum free for 3h at 37°C (99).

3.2.4. Sample Collection

After the appropriate treatments, cell lysates for immunodetection were washed in ice-cold PBS and then collected from each well by pipetting up and down with RIPA lysis buffer (Sigma, cat. #R0278) containing a protease inhibitor cocktail (cOmplete, EDTA-free, Roche, cat. #11873580001). The lysates were sonicated twice during 5 seconds and stored at -20ºC. Protein determination content was perform using BCA assay (see Section 3.4) and normalized protein samples were electrophoretically separated by 5-20% gradient SDS-PAGE gels followed by immunoblotting for the specific protein. Detection was carried out using a chemiluminescence method. The resulting bands were quantified by ChemiDoc Touch Imageing (see Section 3.7).

The adherent cells seeded on coverslips for immunocytochemistry were fixed in Paraformaldehyde 4% (PFA) and subsequently processed for staining as described in section 3.5.

3.3. CSF Sample Collection and Handling

The CSF samples were obtained by means of lumbar puncture in the hospital of Santa Maria da Feira, and aliquots were stored at −80°C until analysis. Then were centrifuged at 3000 rpm for 5min and stored in -80ºC until biochemical assays. Estimation of CSF levels of Aβ42, total TAU and pTAU phosphorylated at threonine-231 and threonine-181 were measured by ELISA, using commercially available kits (Human TAU [pT231] PhosphoELISA™ Kit, Invitrogen; INNOTEST PHOSPHO-TAU [181P] Antigen, Innogenetics; INNOTEST hTAU-Ag, Innogenetics; INNOTEST β-amyloid [1-42], Innogenetics).

3.4. BCA Protein Quantification Assay

Protein quantification of all samples was performed by colourimetric biocinchoninic acid (BCA) protein assay, using Pierce™ BCA Protein Assay kit (Thermo Fisher Scientific, cat. #23225). This assay depends on the capability of protein to reduce Cu^{2+} to Cu^{+} in an alkaline medium (the biuret reaction), which produces a purple-coloured reaction formed by chelation of two molecules of BCA with one cuprous ion. This water-soluble complex exhibits a strong absorbance at 562 nm.

Samples of 5 µl of SH-SY5Y lysates, plasma, serum or CSF were homogenised with buffers (RIPA), directly in the wells (Table 3). Both standards and samples were incubated with 200 µl of working reagent which is prepared with 50 parts of reagent A to 1 part of reagent B. The plate was incubated at 37ºC for 30 min and the absorbance of BCA assay was immediately measured at 562 nm using TECAN Infinite M200.

Table 3. Standards used in BCA protein assay method. BSA: Bovine serum albumin (2 mg/ml); WR, Working Reagent

Standards	BSA (µL)	Buffer (µL)	Protein mass (µg)
P_0	-	25	0
P_1	1	24	2
P_2	2	23	4
P_3	5	20	10
P_4	10	15	20
P_5	20	5	40

3.5. Immunocytochemistry

Immunocytochemistry techniques allow for the detection and localization of antigens in cells and tissues via the use of specific antibodies labelled with fluorochromes (in the case of immunofluorescence). The principle of fluorescence is based on the fact that the electrons are arranged at energetic levels around the atom. Whenever they absorb energy, each electron rises to a higher, less stable energy level. This excited state does not last very long and soon afterwards the electron loses energy in the form of heat and the rest in the form of a photon. There is a range of wavelengths that can excite the electrons of a fluorophore with an optimal peak of excitation for which more fluorescence is produced. The light produced by fluorophores is also represented by a range of values with an optimum emission peak (100).

This technique involves several and crucial steps in order to obtain good final preparations. First samples are prepared by fixing with a fixation agent, this agent helps to stabilize and preserve cells as close to life-like as possible by binding to reactive groups on proteins and lipids and holding them in the same position as if the cells were still alive. The second step is the permeabilization of the cells achieved by the addition of detergents, which can solubilize membranes without destroying the protein-protein interactions. After this cells are blocked, incubated with the chosen antibody and corresponding fluorescent secondary antibody and mounted in a media with anti-fading and anti-photobleaching properties. Finally, the preparation can be visualized through a microscope, and images analysed (100).

SH-SY5Y cells were plated onto coverslips at a confluency of approximately 50%. The cells' differentiation was induced with retinoic acid. The cells were fixed with 4% paraformaldehyde for 10 minutes, permeabilized with 0.2% Triton X-100 for 10 minutes and blocked with PBS 5%BSA for 1 hour at room temperature. Subsequently, cells were immunolabelled with specific antibodies. In order to distinguish between TAUpThr231 and TAU-5, the cells were either labelled with anti-TAUpThr231 monoclonal antibody (Thermo) 1:500 and anti-TAU-5 antibody, mouse (Millipore) at 1:200 in PBS 3% BSA or with anti-TAUpThr231 monoclonal antibody (Thermo) 1:500 and incubated for 3 hours or overnight at room temperature. Primary antibody complexes were visualized using Texas Red Goat anti-Rabbit IgG (H+L) (Molecular Probes) at a dilution of 1:400 and Alexa Fluor® 488 Goat anti-Mouse IgG (H+L) (Life Technologies) at a dilution of 1:300 in 3% BSA in PBS for 1h at room temperature. Coverslips were then mounted onto a microscope glass slides with VECTASHIELD® Mounting Medium for fluorescence, an antifading reagent containing DAPI for nucleic acid labelling (Vectashield, Vector Laboratories) and visualized using an Olympus IX81 fluorescence microscope. Co-localization studies of TAU-5 and TAUpThr231 were carried out by immunofluorescence analysis.

3.6. SDS - Polyacrylamide Gel Electrophoresis

Sodium dodecyl sulfate polyacrylamide gel electrophoresis (SDS-PAGE) is an analytical technique used to separate proteins from a mixture, based on protein molecular weight and charge. The principle of this electrophoresis method relies on the capacity for proteins to migrate through gel pores when placed under an electrical field. The gel percentage and size depend on the molecular weight of the proteins to be separated. As different proteins contain different charges what would interfere with the running, SDS is applied to confer a negative charge to all proteins. One molecule of SDS can bind to two amino acid residues. Therefore, all proteins can migrate from negative to positive anode. SDS is also used in combination with a reducing agent (β-mercaptoethanol) and heat to dissociate proteins before they are loaded on the gel. These reagents cleave disulphide bonds to disrupt tertiary and quaternary protein structures, ensuring protein linearization and equal protein migration in the gel, independently of the three-dimensional structure.

Samples were subjected to 5-20% gradient SDS-PAGE in a Hoefer electrophoresis system. Gels are composed of 2 phases, the non-restrictive large pore called stacking gel and resolving gel with a linear progression of acrylamide concentrations from top to bottom, resulting in a wider separation range. The gradient gel was prepared and allowed to polymerize for 1 h at room temperature. Subsequently, the stacking gel solution was prepared and loaded on the top of gradient gel. A comb was inserted and the gel and left to polymerize for 1 hour at room temperature.

In parallel, samples were prepared by adding to the protein sample solution ¼ volume of 4X LB (Loading Buffer), boiled for 5 minutes. The combs were removed and the gels wells filled with Tris-Glycine running buffer. The samples were carefully loaded into the wells and electrophoretically separated using a 90 mA electric current for 3-4 hours. Molecular weight markers (Precision Plus Protein™ Dual Color Standards, Bio-Rad, cat. #1610374) were also loaded and resolved side-by-side with the samples.

3.7. Western Blot

Western blotting is the technique used for detection of specific proteins in complex samples like cell lysates, cell culture supernatants or body fluids. In this technique, the proteins that were electrophoretically separated by SDS-PAGE can be transferred to a solid membrane (nitrocellulose membranes, for instance), by an electrophoretic field while keeping their positions. This is a fast and efficient procedure and preserves the high-resolution separation of proteins by SDS-PAGE. Once in the membrane, proteins are suitable for detection by total protein staining or labelling the proteins of interest with specific antibodies (101).

After SDS-PAGE gels proteins were electrophoretic transferred to nitrocellulose membranes in a wet system for 18h and at 200 mA. The transfer was further confirmed using Ponceau staining solution, which is a red stain dissolved in an acidic solution. Ponceau S binds to protein positive amino acids and to non-polar protein regions in a non-covalent form. The membrane was hydrated with a Tris-buffered saline solution (TBS) during 10 min with agitation and, then, Ponceau staining solution was applied during 5 min with agitation. After this incubation, the solution was removed and the membrane was washed with deionized H_2O to remove the excess of ponceau solution (101).

For immunodetection, after total Ponceau removal, membranes were blocked in 5% BSA in 1x TBS-T (0.5% Tween-20), at RT during 4 hours, to inhibit possible non-specific binding sites of the primary antibody. Membranes were incubated with primary antibody in 3% BSA extract solution for 4 hours with agitation at room temperature plus overnight at 4°C. Membranes were washed with TBS-T six times for ten minutes and then incubated with the appropriate secondary antibodies coupled to horse radish peroxidase (HRP) for 2h at room temperature. The membranes were washed five times for ten minutes each with 1x TBS-T.

Protein bands were detected using the chemiluminescence reagent Amersham ECL Select Western Blotting Detection Reagent (GE Healthcare Life Sciences). Enhanced chemiluminescence (ECL) reagent is based on luminol substrate oxidation by HRP, generating chemiluminescence at 425 nm. The emitted light is directly proportional to the amount of protein. The membranes were incubated for 5 min with the working mixture of the chemiluminescent detection reagent, at room temperature. Images were exposed between 1 min and 30 min and the resulting image was observed in ChemiDoc Imageing System.

3.8. Enzyme Linked Immuno Sorbent Assay

The Enzyme Linked Immuno Sorbent Assay (ELISA) method is a potent method for detecting and quantifying a specific protein in a complex mixture as it allows for analysing protein samples immobilized on a microplate using specific antibodies.

A solid-phase sandwich ELISA (Human TAU [pT231] PhosphoELISA™ Kit, cat. # KHB8051, Invitrogen) assay was used to detect TAU phosphorylated at Thr231 (PTAU231). The ELISA sandwich is used for more complex protein samples since only the antigen of interest is immobilized on the antibodies, the capture antibody and the detection antibody. All reagents used were supplied in the kit including the "standards dilution buffer". Wash buffer was prepared by diluting the supplied concentrate 1:25 with purified water.

Standards were prepared by diluting the supplied standard with "standard dilution buffer" as specified on labelling to 100 U/mL. The standard curve was constructed by 8 double down dilutions starting at a content of 50 U/ml down to 1.56 U/ml, plus a 0 point. The calibrator used for the assay was a recombinant Hu TAU-441 expressed in E. coli and SMCC conjugated to phospho-peptide T231.

A specific TAU monoclonal antibody was coated onto the wells of a 96-well plate. During the first incubation, 100 µL of standards of known TAU [pT231] content and samples were added to each well and the TAU antigen bind to the immobilized (capture) antibody. The ELISA plate was covered and incubated for 2 hours at room temperature on a shaker. After washing, a rabbit antibody specific for TAUpThr231 was added to the wells. The plate was incubated as above for 1 hour and thereafter washed 4 times. During the second incubation, this antibody served as a detection antibody by binding to the immobilized TAU protein. After washing, we added a horseradish peroxidase labelled anti-rabbit IgG that binds to the detection antibody, and the plate was incubated for 30 minutes at room temperature. After a third incubation and washing to remove all the unbound enzyme, a stabilized chromogen (TMB) was added, which binds to the enzyme to produce colour. The uncovered plate was incubated at room temperature in the dark for 30 minutes. The reaction was completed by the addition of a provided "stop" solution, and the plate was then read at 450 nm in a Tecan microplate reader. The intensity of this coloured product is directly proportional to the concentration of TAU [pT231] present in the original specimen and the optical density can be read on a standard microplate reader.

Phospho-TAU (181P), Total TAU and Amyloid-β (Aβ42) levels were measured using commercially available ELISA microplate assay (Innotest®, Innogenetics, Ghent, Belgium).

3.9. Albumin Depletion

3.9.1 Albumin/IgG using ProteoSeek columns

Plasma samples for immunoblotting were stripped of Albumin/IgG using ProteoSeek columns (IgG removal kit, Thermo Sci, cat. #89875). This is a high capacity kit that uses an immobilized Cibacron Blue dye agarose resin capable of binding with a variety of species-specific albumins. This is placed in the Pierce Spin Columns and by low-speed centrifugation, the albumin binds to the resin making possible its removal from the samples.

3.9.2 Immunoprecipitation

Immunoprecipitation (IP) is a technique in which a target protein, antigen or protein complex is precipitated from a solution using a specific antibody. It is widely used to estimate molecular weight, identity, quantity and expression levels of a protein of interest and to study protein-protein interactions.

The magnetic DynaBeads are the solid support used in our immunoprecipitation approach. The immunecomplexes attached to DynaBeads are easily removed from the supernatant by magnetic separation. The pure precipitate can then be eluted from the beads and analyzed by western blotting or mass spectrometry. In this specific case, DynaBeads are coupled to protein G that has different affinity to Ig's of different species.

After BCA protein quantification (see Section 3.4), normalized samples were pre-cleared with 15µL Dynabeads® Protein G (Thermo Sci, cat. #10004), for 1 hour at 4ºC with rotation. DynaBeads Protein G was previously washed twice with 3% BSA/1x PBS. Subsequently, the supernatant was transferred to a new microtube that contained 40 µL DynaBeads conjugated with the specific primary antibodies (TAU Total, dilution 1:100) and incubated overnight at 4ºC with rotation. Further, the supernatant was transferred to a new microtube and the DynaBeads washed three times with 3 % BSA/1x PBS and three times with 1x PBS (10 minutes each, at 4ºC with agitation). Finally, DynaBeads were re-suspended in 100 µL of 1x Loading Buffer and boiled at 70ºC for 10 min.

3.10. Quantification and Statistical analysis

Image Lab™ Software 6.0 (Bio-Rad) was used to quantify band intensity and correlate it to protein levels. The Shapiro-Wilk normality test was used to assess the normality of distribution of investigated parameters. Difference between groups was established using ANOVA. The unpaired t-test was used to compare means and correlation analyses were performed using Pearson's test. The values $P < 0.05$ were considered statistically significant. Statistical analyses were performed using IBM SPSS Statistics V22.0. Plots were made using the GraphPad Prism version 7.00 for Windows, GraphPad Software (La Jolla, California, USA).

Quantification of colocalization was performed using Image J (NIH) in individual frames after thresholding, and colocalization was calculated with the JACoP plugin of the same program in merged images.

4. Results

4. Results and discussion

4.1 SH-SY5Y cells and PhosphoTAU231

4.1.1 Aβ effects in TAU phosphorylation

In order to mimic AD, aggregated Aβ42 peptide was added at increasing concentrations (2, 10 and 20μM) for 3 hours to undifferentiated and differentiated SH-SY5Y cells, as explained in section 3.2.1. Following this incubation period, the cell lysates were collected and further analysed by immunoblotting using TAU-5, TAUpThr231, β-Tubulin and Actin antibodies. β-Tubulin was used as differentiation control and Actin was used as loading control.

When the SH-SY5Y cells undifferentiated and differentiated were incubated with increasing concentrations of aggregated Aβ42 for 3 hours, there seemed to be no significant changes in TAU levels with Aβ42 (Figure 8A), but it is significantly increased with differentiation (P=0.025). In the same experimental set, tubulin appears to be increasing with the differentiation (Figure 8A).

(A)

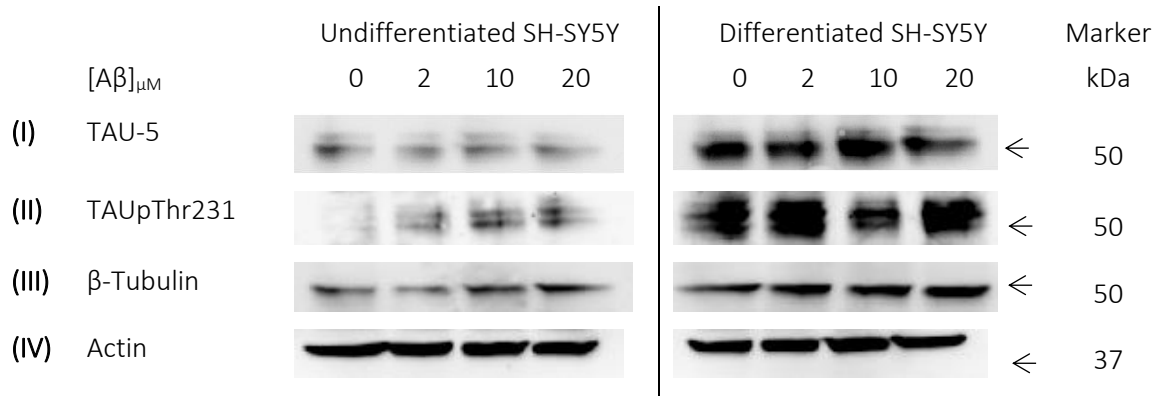

(B)

(I)

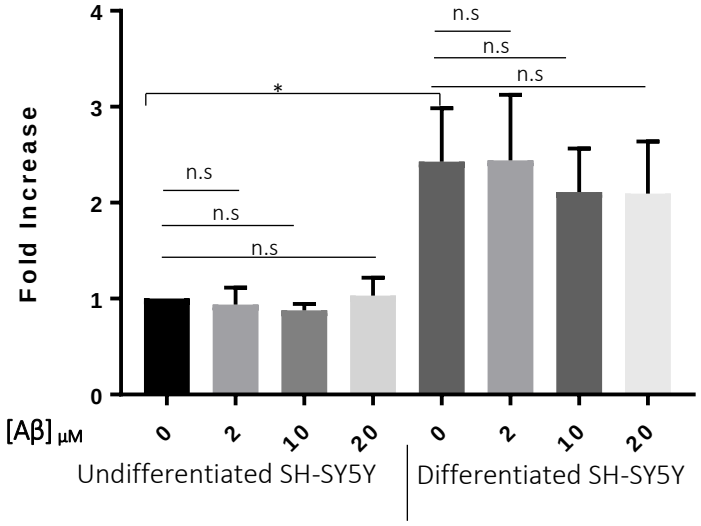

TAU-5

(II)

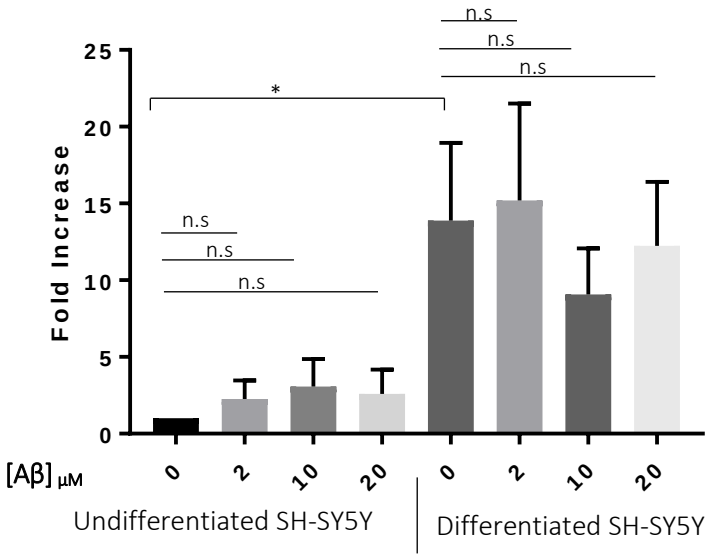

TAUpThr231

(C)

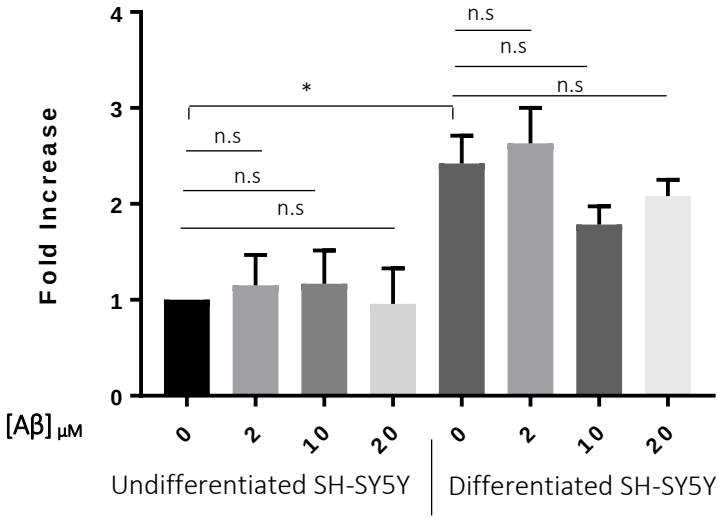

Ratio Thr231/TAU

*Figure 8. Effects of Abeta on TAU phosphorylation at Thr231 residue. Differentiated and undifferentiated SH-SY5Y were incubated for 3 hours with aggregated Aß42 (2, 10 and 20 µM) A. Cells lysates were collected and protein levels of TAU-5 (I) and TAUpThr231 (II) were analysed. ß-Tubulin was used as a loading control (III) B. The expression levels of TAUpThr231 (I) and TAU-5 (II) were measured. C. Quantification of TAU phosphorylation at Thr231 were normalized to Total TAU content. The undifferentiated control was set at 1 and the fold increase/decrease was calculated. All data represent means ± SEM. Data were obtained from triplicate experiments. The relation between groups was calculated using the unpaired Student's t-test, * P < 0.05*

Relative to the TAU phosphorylation, more specifically at the Thr231 residue the levels were very similar with the concentration of Aβ, but there was a significant increase in the phosphorylation in the differentiated cells when compared with the undifferentiated SH-SY5Y cells in the control (p=0,029). This may indicate that the phosphorylation of the Thr231 residue is not due to increasing Aβ but may be a relevant process associated with cell differentiation.

In order to have a clearer idea of the phosphorylation pattern on this residue, following Aβ 1-42 treatment the ratio of phosphorylated TAU protein (pTAU) versus total TAU protein (total TAU) was calculated (Figure. 8C). The analysis of this ratio revealed that TAU phosphorylation upon Aβ42 treatment at Thr231 does not have significant differences when Aβ42 is added for 3 hours, but there is still a significant increase in the phosphorylation in the differentiated cells when compared with the undifferentiated SH-SY5Y cells in the control (p=0,049).

To see if the tendency to increase phosphorylation when cells are differentiated is specific for this residue, we tested other TAU phosphorylation sites (Ser262, Ser369) as well as another microtubule-associated protein, MAP2. Total TAU and Tubulin were included as controls.

A

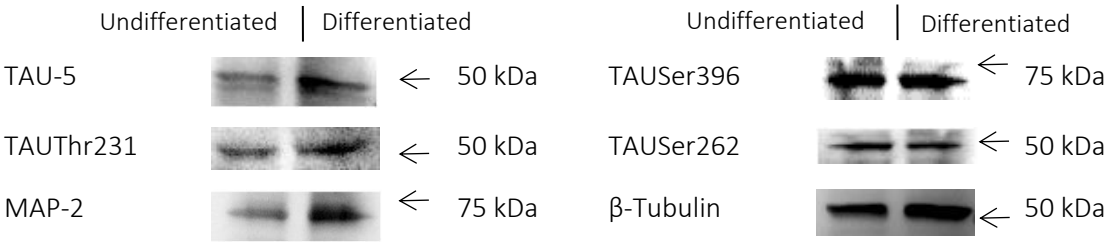

B

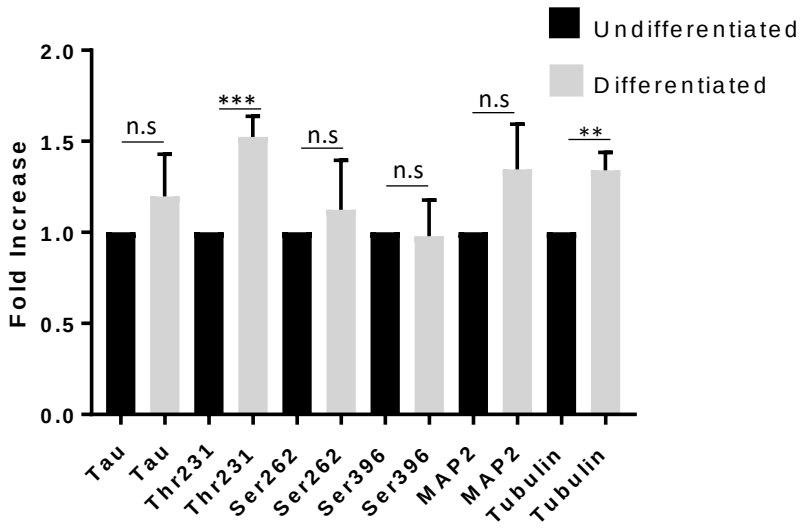

*Figure 9. Differences in protein expression in undifferentiated and differentiated SH-SY5Y A. Cells lysates were collected and protein levels of phosphoTAU231, TAU-5, phosphoTAU262, phosphoTAU369, MAP2 and β-Tubulin were analysed by Western blot. B. The expression levels were measured. All data represent means ± SEM. Data were obtained from triplicate experiments. The relation between groups was calculated using the unpaired Student's t-test, ** P < 0.01, *** P<0,001*

There were no apparent differences in phosphorylation levels at the TAU phosphorylation sites tested, apart from Thr231, which was significant ($P < 0.001$). Additionally, there was a tendency for MAP2 and TAU levels to increase with differentiation. Tubulin was significantly increased ($P = 0.002$).

4.1.2 Phospho TAU 231 localization

Changes in the subcellular distribution and conformation of TAU during the progression of Tauopathies have been studied in an attempt to understand the process of neurofibrillary tangle (NFT) formation.

To this end, SH-SY5Y neuroblastoma cells were differentiated with RA for five days into neuron-like cells displaying morphological and biochemical features of mature neurons, as described in the methods. Contrast-phase photographs were taken to visualize morphological differences in undifferentiated and differentiated cells (Figure 10).

Undifferentiated

Differentiated

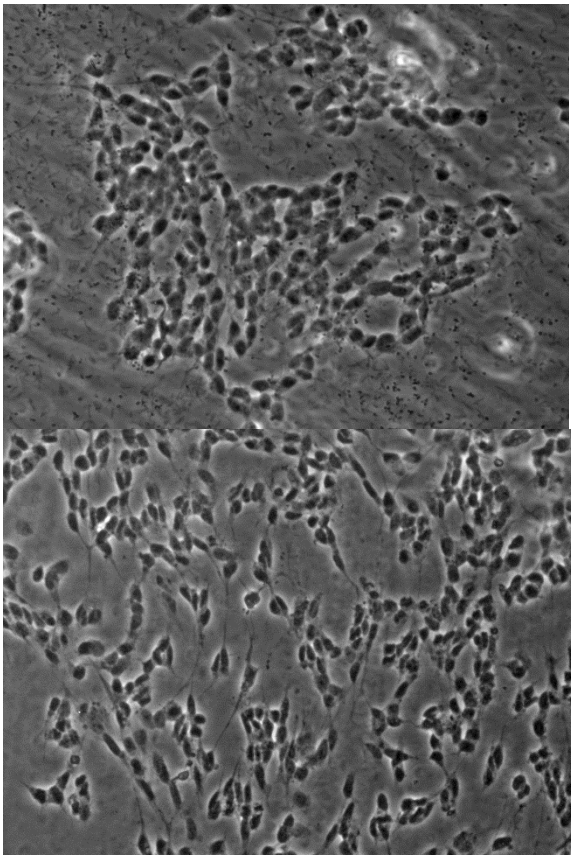

Figure 10. Differentiation of SH-SY5Y cell line, (Scale Bar = 100 µm).

Undifferentiated SH - SY5Y cells tend to grow in clusters and may form clumps of rounded cells on top of one another. Differentiated SH - SY5Y cells do not cluster. The differentiated SH-SY5Y cells have an apparent neuronal morphology with more elongated phenotype and extensive neurite outgrowth, reminiscent of dendrites and/or axons.

In this study, we examined the intracellular distribution of total TAU and TAUpThr231 in undifferentiated and RA-differentiated SH-SY5Y cells (Figure 11) by immunocytochemical staining using mouse monoclonal antibodies against TAU-5 and anti-TAU pT231, respectively.

In both undifferentiated and differentiated SH-SY5Y cells, total TAU is mainly located in the cytosol (Figure 11).

Undifferentiated neuroblastoma SH-SY5Y cells predominantly expressed pTAU231 proteins at the nucleus, while after RA-differentiation TAUpThr231 immunostaining was also found in the cytosol and along the neuritic processes (Figure 11).

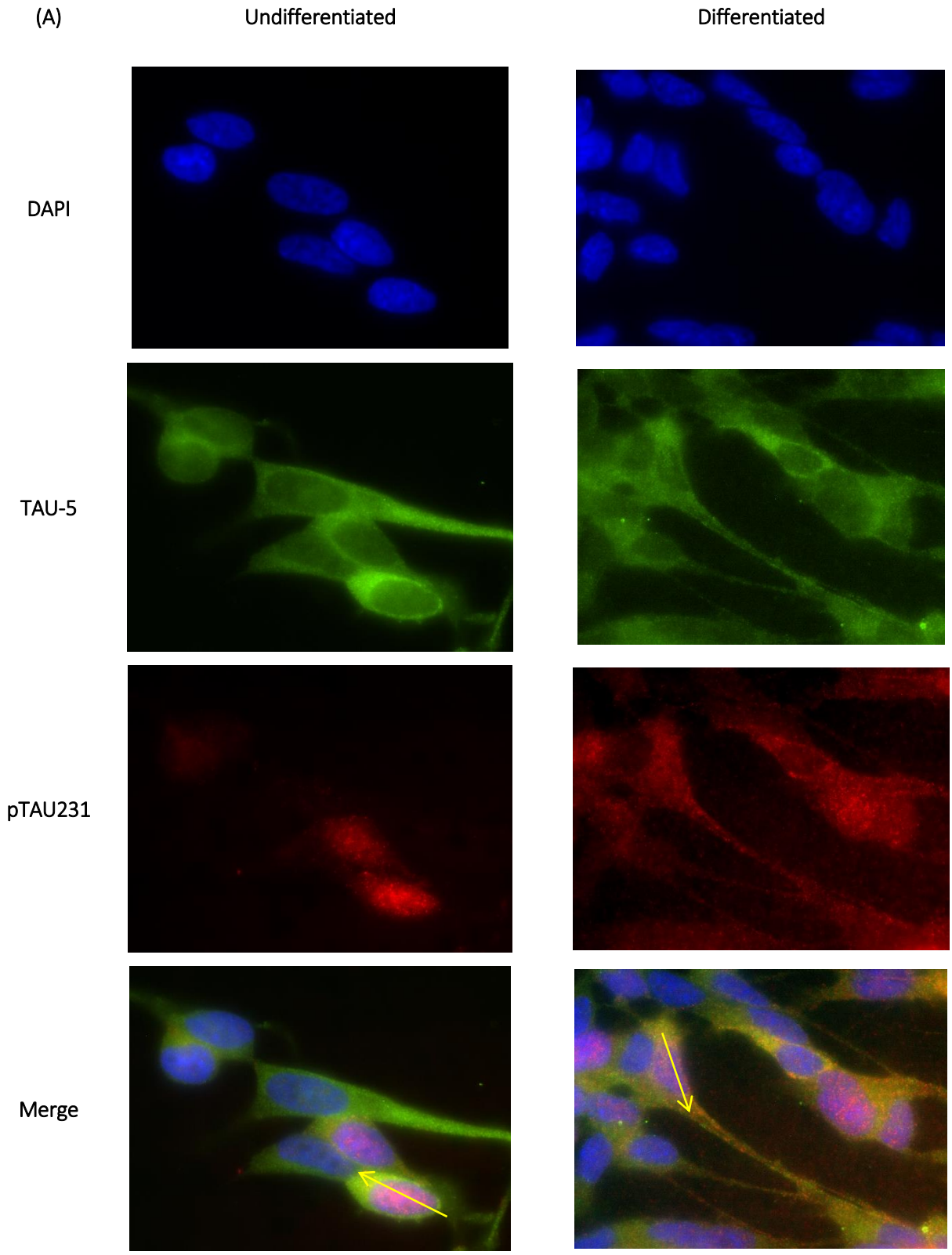
(A)
Undifferentiated
Differentiated
DAPI
TAU-5
pTAU231
Merge

(B)

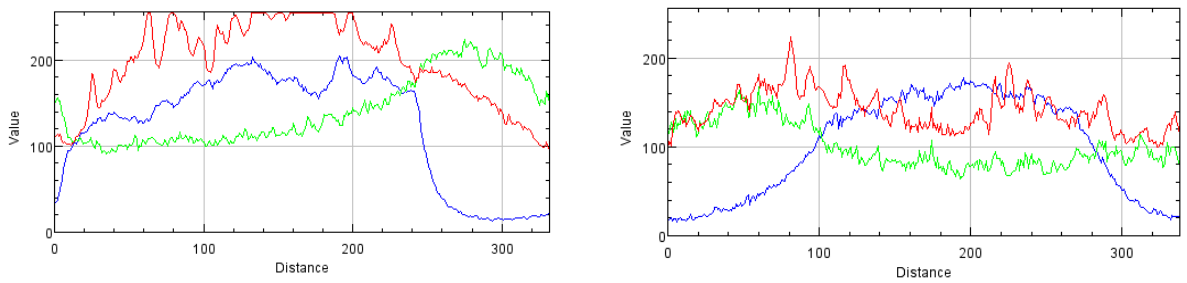

Figure 11. Total and TAUpThr231 protein distribution in undifferentiated and RA-differentiated SH-SY5Y cells. (A) Co-immunostaining for TAUpThr231 (red staining) and TAU-5 (total TAU-green staining) showed no detectable overlap in the undifferentiated cells. TAUpThr231 localized mainly in the nucleus. TAU protein distributed along the cytosol of undifferentiated SH-SY5Y cells. RA treatment shifts the distribution of Total and Phosphorylated TAU protein into the neurites (B) Representative staining profiles. Left-undifferentiated cells, right-differentiated. Fluorescence intensity profiles represent the voxels through the white lines indicated in the merged image shown in A. (Scale Bar = 20 µm).

In the undifferentiated SH-SY5Y cells most TAUpThr231 localized to the cell nuclei. Co-immunostaining for TAUpThr231 and TAU revealed slight overlap in the cytosol. Induction of differentiation using RA resulted in neurite formation and a shift in TAU distribution from soma to neurites (Figure 11A). We found, as demonstrated in the fluorescence profile, that the level of phosphorylated TAU decreased in the nucleus (DAPI-positive organelle) after the differentiation treatment of SH-SY5Y with retinoic acid, and became detectable in the cytosol and along the processes (Figure 11B). Hence the blue trace (labels the nucleus) is sustained with RA exposure, whereas the red trace for TAUpThr231 drops, to similar values of those of the green trace for t-TAU. Of note, this analysis was carried out in non-apoptotic cells, as denoted by nucleus morphology (DAPI staining). This finding may suggest that the translocation of pTAU from the nucleus to the cytosol is part of the differentiation program.

The co-localization of TAU and TAUpThr231 with DAPI was analysed to see their percentage of nuclei localization (Table 4).

Table 4. Percentage of protein localized in the nuclei. Data is presented as mean±SD of a of minimum 20 analysed cells of each condition

	TAU	T231
	Mean (SD)	Mean (SD)
Undifferentiated	31.21 (16.99)	54.88 (28.97)
Differentiated	24.27 (10.19)	39.56 (25.7)

There is a significant decrease in the percentage of TAUpThr231 localizing in the nuclei of differentiated cells when compared with undifferentiated cells (P=0.018).

Finally, we analysed the percentage of co-localization among the previous proteins (Figure 12). Colocalization coefficients of Manders (M1 and M2) represent the percentage of a protein colocalizing with the other. When both coefficients are equal to 100, there is a perfect co-localization. In this case, M1 represents the percentage of TAUpThr231 that co-localizes with TAU and M2 represent the percentage of TAU that co-localizes with TAUpThr231. TAUpThr231 colocalization with TAU significantly increased with differentiation (P=0.002).

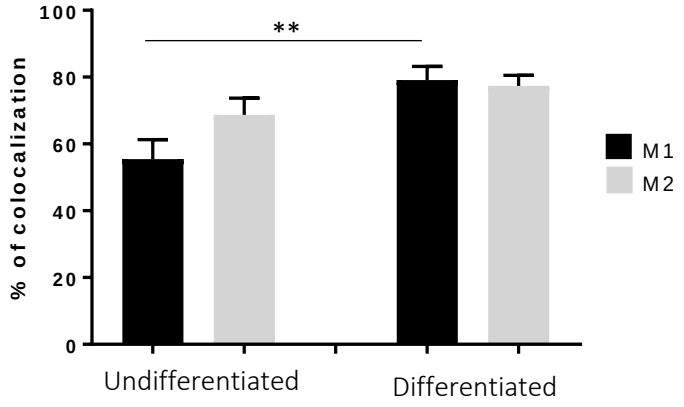

*Figure 12. Percentage of co-localization distribution of T231:TAU in undifferentiated and RA-differentiated SH-SY5Y cells. Data is presented as mean±SEM of a of minimum 20 analysed cells of each condition.*P<0,05, **P<0,005*

4.2. Optimizing TAUpThr231 detection in Human Samples

The use of CSF biomarkers, despite being good predictors of AD, is hampered by a high degree of invasiveness, requires a lumbar puncture, has high costs, and availability is limited. Biomarkers based on standard blood tests represent several advantages. Results based on research would allow for efficient monitoring of disease processes in AD and could be used as a screening tool in primary health care. Thus this section addresses analysing human blood samples for putative AD biomarkers.

Proteomic-based approaches are being sought with respect to blood-based diagnostics. However, the use of proteomics for efficient, accurate, and complete analysis of clinical samples poses a variety of technical challenges. The presence of higher abundance proteins in the plasma, such as Human serum albumin (HSA), may mask the detection of lower abundance proteins such as TAU, as it often accounts for greater than 60% of the total protein present in serum samples.

A number of different strategies have proved efficient in selectively extract therapeutic proteins from this albumin reach plasma/serum samples. These approaches includes techniques, such as albumin depletion using plates or columns and immunoaffinity purification using antibodies. In our study, in order to remove Albumin/IgG from the plasma and serum samples, ProteoSeek columns were used. Protein content was determined by BCA protein assay Kit (Pierce, Rockford, IL, USA). Then the proteins in the samples were separated by SDS-page followed by Western Blot procedures. With the BCA method it was visible that the protein content diminished significantly after being subjected to the ProteoSeek columns but after the incubation with TAUpThr231 antibody, we could not be sure that the band detected corresponded to TAUpThr231 or if it was still Albumin (data not shown). Also, this columns may result in the removal of other proteins other than albumin, and as the initial volume is only 10 µL and TAU in blood in in small quantity, this may not be the best solution.

In a different approach, an immunoprecipitation with Dynabeads in plasma and serum samples was used to isolate total TAU-5 protein. The immunoprecipitates were then separated by SDS-page followed by immunoblotting using TAUpThr231 antibody. The interference of several blood abundant proteins was still extremely evident and we could not detect the TAUpThr231 band (data not shown).

Given that one could not accurately detect TAUpThr231 by Western Blotting, we tried to determine the levels of TAUpThr231 in plasma, serum and CSF samples with a Human TAUpThr231

ELISA Kit. This kit did not detect significant levels in plasma nor serum but had positive results in CSF (Table 5).

Table 5. Human TAUpThr231 ELISA Kit test results in several human fluids

Sample	Abs (562 nm)$_{med}$	Protein Content (µg)
Serum	0,0893	1,57
Plasma	0,0877	1,52
CSF	0,1732	4,22

Therefore, to determine how the degeneration of brain cells containing hyperphosphorylated TAU in AD is reflected in the CSF, TAU phosphorylated at Thr181 and Thr231, Total TAU and Aβ42 were quantified using several immunoassays using CSF samples of human patients, as described in section 3.9. A total of 50 samples were divided into 3 groups, according to their neurochemical and psychological diagnosis (the ELISAS for TAUpThr181, t-TAU and Aβ42 had been previously carried out, Henriques et al, personal communication).

In the CSF samples, we observed that the levels of Aβ peptide were significantly decreased in the AD group when compared to the non-AD group ($P<0.0001$) (Figure 13A). In contrast, the levels of t-TAU protein significantly increased in patients with AD when compared with the non-AD group ($P<0.0001$) and with the amyloid pathology group ($P<0.0001$) (Figure 13B). TAUpThr181 is also increased in CSF samples of AD patients when compared to non-AD ($P<0.0001$) and positive Aβ samples ($P<0.0001$) (Figure 13C). TAUpThr231 did not have statistically significant changes ($P=0.33$) (Figure 13D).

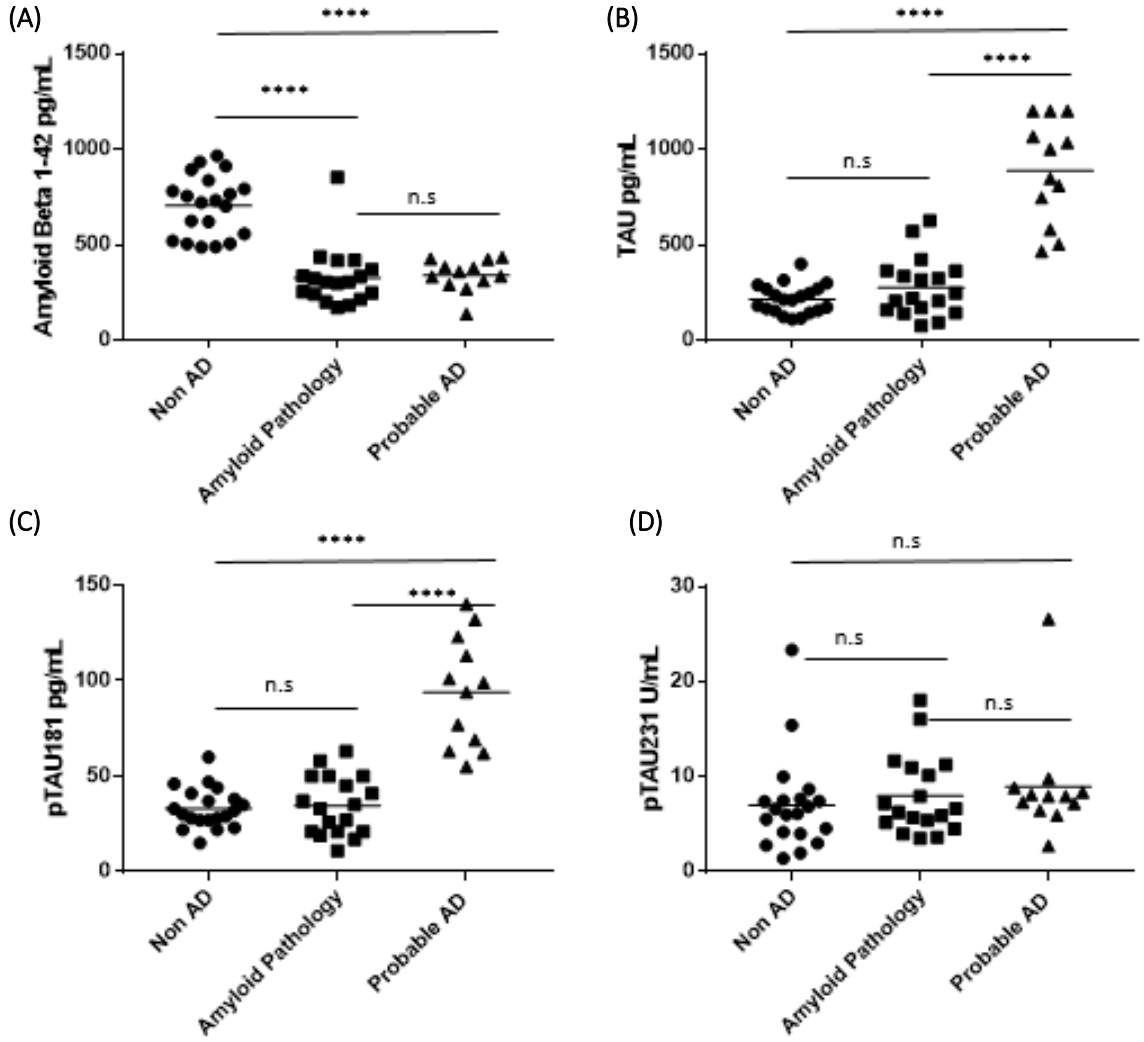

*Figure 13. Aβ, TAU and TAU phosphorylation levels in CSF samples. CSF samples of AD negative, Aβ positive and AD patients were assayed using specific ELISA kit for Aβ peptide (A), total TAU (B), TAUpThr181(C) and TAUpThr231 (D). The relation between groups was calculated using the unpaired Student's t-test, **** P < 0.001*

In order to have a clear idea of the phosphorylation pattern on these residues, the ratio of phosphorylated TAU protein (pTAU) versus total TAU protein (total TAU) (Figure 14) was calculated.

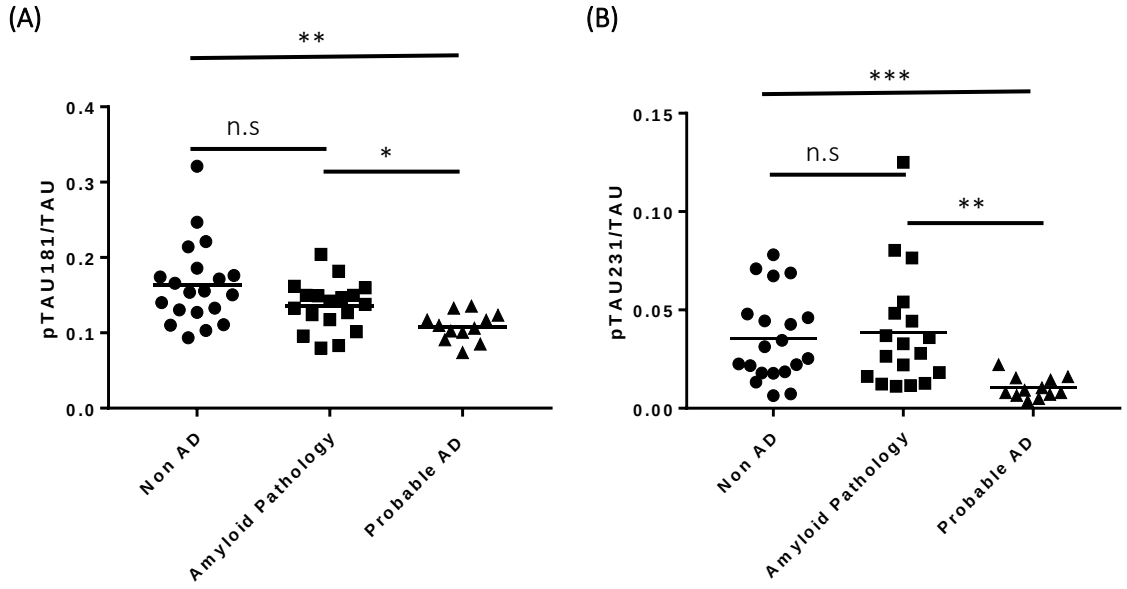

*Figure 14. Phospho TAU and TAU ratio. CSF levels of PTAU normalized against levels of total TAU (PTAU to t-TAU ratio).The ratio of the phospho TAU with the total TAU were calculated. The PTAU to t-TAU ratio in AD CSF was significantly lower than the other groups. The relation between groups was calculated using the unpaired Student's t-test, ***P < 0,001; **P < 0,005; *P < 0,05.*

The analysis of this ratio revealed that both TAU phosphorylation in Thr181 (P = 0,002) and Thr231 (P < 0,001) exhibits a tendency to significantly decrease in AD positive patients compared with non-AD and patients with amyloid pathology. Moreover, TAUpThr231/t-TAU ratio levels seemed to improve diagnostic accuracy compared with TAUpThr181/t-TAU ratio levels in patients with AD.

To evaluate the diagnosis significance to discriminate AD from non-AD individuals of both ratios, we did a ROC curve (Figure 15). The curves were constructed by computing the sensitivity and specificity of the ratios. If the area under the ROC curve is closer to 1, you have better test. Both ratios were considered to be "good" at discriminating between Alzheimer's disease patients and non-AD. We found that the diagnosis performed more accurately in T231 ratio (area under the curve = 0.89, SD=0.060, 95% CI: 0.73 to 0.97) compared to T181 ratio (area under the curve = 0.86, SD=0.063, 95% CI: 0.70 to 0.96). These differences however were not statistically different (P = 0.777).

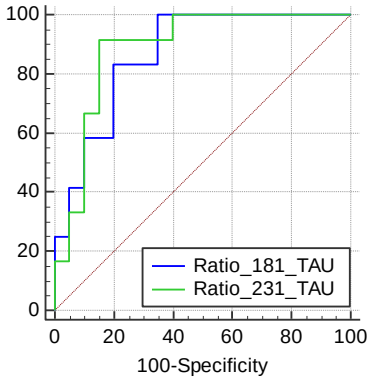

Figure 15. ROC Curve analysis of the sensitivity and specificity of both phosphoTAU/TAU ratios as discriminators of AD and Non-AD individuals

Other relevant characteristics of the study group are summarized in table 4 to better analyse the relationship between some relevant variables analysed.

Table 6. Characteristics of the study population. P-Values calculated with ANOVA.

Variable	Non-AD (N=20)	Amyloid Pathology (N=18)	Probable AD (N=12)	P Value
Age (years)	64.4 (56-77)	71.1 (46-85)	70.1 (57-85)	0.06
Female, No. (%)	55	67	50	0.43
ApoE ε4 genotype (0/1/2), No	19/1/0	11/6/1	7/2/3	0.11
CSF Aβ42, mean (SD), pg/mL	704.5 (155.02)	327.44 (149.64)	339.58 (79.80)	<0.001
CSF TAU, mean (SD), pg/mL	214.50 (74.58)	275.94 (149.60)	887.25 (259.65)	<0.001
CSF TAUpThr181, mean (SD), pg/mL	34.16 (9.70)	33.20 (10.34)	94.00 (27.77)	<0.001
CSF TAUpThr231, mean (SD), U/mL	7.01 (4.84)	7.99 (4.08)	8.93 (8.59)	0.26
Ratio Thr181/TAU, mean (SD)	0.16 (0.05)	0.14 (0.03)	0.11 (0.02)	0.002
Ratio Thr231/TAU, mean (SD)	0.04 (0.02)	0.04 (0.03)	0.01 (0.01)	0.005

The association between the studied proteins and age were analysed. As the samples followed a normal distribution, Pearson correlation coefficient was used. None of the proteins analysed (Aβ42, TAU, T181, T231) displayed any correlation with age (P = 0.078, 0.733, 0.765, 0.324 respectively). The ratio of Thr181 with TAU and Thr231 with TAU did not correlate either (P = 0.210, P = 0.919, respectively)

Within the AD set was 4 early-onset AD patients (younger than 65 years). Statistical analysis did not reveal a significant difference in phospho-TAU231 levels between the early-onset and late-onset AD patients (P = 0.22) nor with the Thr231/TAU ratio (P = 0.99). Thus, age does not appear to be a significant factor for TAU Thr231 phosphorylation levels in CSF.

In relation to gender, we also saw no correlation with any of the proteins age (P = 0.078, 0.733, 0.765, 0.324 respectively).

We looked for statistical interactions between the analysed proteins level and ApoE ε4 genotype carriers and gender, and concluded that there was a significant correlation between Aβ42, TAU and TAUpThr181 (P = 0.011, 0.010, 0.004, respectively) but not with TAUpThr231 (P = 0.604). The correlation of both ratios with ApoE was also analysed and again only Thr181/TAU was statistically significant (P = 0.032).

While analysing the ApoE ε4 genotype of each group we noticed, as expected, that there is a significant difference between the AD group and non-AD group (P < 0.001), and between the Amyloid Pathology group and non-AD group (P = 0.011).

5. Discussion

5. Discussion

5.1 PhosphoTAU231 in SH-SY5Y cells

In this study, we examined the putative function TAUpThr231 and how that might affect the protein's localization in SH-SY5Y neuroblastoma cells. The value of TAUpThr231 as a potential AD biomarker was investigated. We addressed the effects of Aβ on TAU phosphorylation of this residue and found that the phosphorylation levels did not fluctuate with exposure to Aβ. However, significant differences in basal TAUpThr231 and total TAU levels were shown in both undifferentiated and differentiated SH-SY5Y cells. This may indicate that the phosphorylation of Thr231 is not due to an increase of Aβ, but may be a relevant process in cell differentiation. TAU has been suggested to increase with cell differentiation as the expression of all six mature TAU isoforms are used as markers for adult neurons (103). A previous study found in a Western blotting analysis obtained from hippocampal neurons samples that after Aβ42 oligomer exposure, TAU Thr231 phosphorylation decreased within the first 3–8 h, returning to control levels within 24 h (104). There are studies on other TAU phosphorylation residues, Ser262 and Ser396, where an increase in expression of both phosphorylated proteins was observed (105).

To see if this phosphorylation pattern was common to other TAU phosphorylatable residues, TAUpSer262 and TAUpSer369 were tested. The latter are all relevant AD epitopes since they are reported to be hyperphosphorylated at an early stage of AD. No significant changes were detected upon cell differentiation. Thus of the TAU residues tested only Thr231 increased with differentiation. Alternatively, treatment with RA in SH-SY5Y was previously shown to increase total TAU and TAU phosphorylated at Ser199, Ser202, Thr-205, Ser396, and Ser404 protein levels, all of which are hyperphosphorylated in Alzheimer's Disease (106,107), but decrease the expression of TAU phosphorylated at Ser262 (108). Furthermore, protein levels of MAP-2 and β-Tubulin, all microtubule-associated proteins, were shown to increase with cell differentiation. These proteins have been previously identified as indicators of differentiation (109).

5.2 PhosphoTAU231 cellular localization

Colocalization studies of TAUpThr231 with t-TAU in undifferentiated and differentiated SH-SY5Y cells were carried out in this study. The differentiation of SH-SY5Y cells results in a cell population that is both morphologically and biochemically distinct from undifferentiated SH-SY5Y cells with apparent neuronal morphology with extensive neurite outgrowth. The majority of TAU localize in the cytosol. A previous study found that traditionally cultured cells treated with RA for 7 days display poor TAU staining, mainly localized around the nucleus (103).

It is important to note that the expression levels and cellular localization of TAU are different in human adult brain neurons when compared to cultured cells. Thus, in mature neurons, TAU is mainly found in the axons whereas, in cultured cells, such as in this study, TAU is present throughout the cells including the cell soma (110). This intracellular localization of TAU has been also reported in other studies (103,108,111).

In undifferentiated cells, TAUpThr231 has a preferentially nuclear localization and in differentiated cells its localization expands to the cytosol and neuritis, suggesting that it may be part of the differentiation program. PhosphoTAU co-localized with t-TAU especially in differentiated SH-SY5Y cells. This co-localization reinforces the hypothesis that TAUpThr231 is translocated from the nucleus to the soma and neurites of SH-SY5Y cells with differentiation since the total TAU is located mainly outside the nucleus, as was previously mentioned (103).

5.3 TAUpThr231 levels in Human Sample

The relevance of TAUpThr231 in human samples, as a potential biomarker, was addressed in plasma, serum and CSF. The ideal fluid to access biomarkers is blood because it circulates through all the organs and contains secreted proteins. In addition, the collection of blood is not as invasive as a lumbar puncture. Unfortunately, we could not efficiently detect the TAUpThr231 residue in neither plasma nor serum because of the interference of several blood abundant proteins, such as albumin, that masked our protein of interest even after several clearance procedures

CSF analyses proved to be a better procedure for identifying TAUpThr231. While analysing a set of 50 CSF samples of AD and non-AD patients, we observed that the ratio of TAUpThr231/t-TAU levels significantly differentiated the AD group from the non-AD group. Moreover, TAUpThr231/t-TAU ratio levels improved diagnostic accuracy in patients with AD compared to the commonly used pTAU181/t-TAU ratio levels. In accord with our findings, a study performed by Spiegel et al, showed that pTAU231 was superior to pTAU181 in the separation of AD from normal controls. Also, that the major performance difference between the two residues was found in the greater accuracy of pTAU231 in the classification of cognitively normal subjects yielded significantly fewer false positives (112). The relationship of Thr231 phosphorylation levels and of the ratio of Thr213/TAU with age, ApoE genotype and gender were also analysed and no significant correlation with neither of this variables was evident. These findings indicate that TAUpThr231/t-TAU ratio levels may be a valuable marker for the clinical diagnosis of AD, irrespective of age and gender.

In these same CSF samples, Aβ peptide was found to be decreased in AD patients. A study found that the presence of cortical amyloid plaques was associated with lower levels of CSF Aβ42. The lower CSF levels of Aβ42 in AD patients compared with controls are believed to be caused by its accumulation in senile plaques, a classical hallmark in Alzheimer disease (113). In addition, high protein levels of total TAU and TAU phosphorylated at Thr181 are observed in patients with AD. Total TAU has been successfully analysed in CSF since 1995, showing a significantly elevated concentration in AD patients compared with controls as well as in patients with other neurodegenerative disorders (114). Tau and Aβ in CSF represent the earliest and most intensively studied biomarkers. The decrease of CSFAβ42 and increase of TAU proteins are currently accepted diagnostic biomarkers of AD (35,115). Given that hyperphosphorylation of TAU is associated with the formation of NFTs, the increase seen in CSF samples of AD patients may indicate the presence or formation of tangles in AD patients.

The data in this report supports the analysis of the levels of phosphoTAU in CSF as a diagnostic biomarker for AD. Over the years, CSF levels of several epitopes of tau protein have been analysed by ELISA to determine potential biomarkers. Kohnken et al and Buerger et al both showed that Thr231 could discriminate between patients with AD and control subjects with an extremely high specificity (87,93). Other studies show the levels of Thr231 together with other residues such as Thr181 and Ser235, reporting that phosphorylated CSF -TAU levels were significantly higher in AD patients than those in non-AD controls (112,114,116).

5.4 Future prospects and Challenges in biomarker discovery

Future research and improvements can be made as the present study has several weaknesses and challenges given that our clinical AD sample size was relatively small and did not include subjects with other relevant conditions such as mild cognitive impairment. There are still some crucial issues that need to be improved in order to achieve an optimal implementation of CSF biomarkers in clinical trials. On one hand, more observational longitudinal studies with larger sample sets are needed to determine the patterns of biomarker change along the natural course of the disease. Another constraint is the low concentration of TAU in CSF, ranging from approximately 300 ng/L in healthy individuals to 900 ng/L in AD patients, falling close to the detection limit of most assays (117).

In terms of cell culture, the future work arising from these studies may be to use different incubation times with Aβ peptide (0 to 24h) to better see its influence in the phosphorylation of TAU. Also, to use different time points in the differentiation program to see in which the translocation of the phosphorylated TAU happens.

The challenges we faced were mostly during the blood analysis. Blood is comprised of multiple cellular compartments and an ever-changing environment of proteins, lipids, and other biochemical entities such as albumin, heparin or ethylenediamine tetraacetic acid (EDTA) that can impact biomarker stability and detectability. Several albumin removal methods should be used during the examination of serum and plasma protein content. Affinity chromatography techniques and trichloroacetic acid precipitation along with the methods based on the columns containing specific resin to remove albumin and immunoglobulin increases the chance to observe the proteins which are naturally in serum binding to albumin and globulins on the protein pattern (118). It is noteworthy that most of the work within the AD blood-based biomarker space remains in early discovery stage with only a few laboratories replicating across cohorts and even fewer attempting to

lock down methods for prospective studies. Several groups have identified promising signals in peripheral blood, suggesting that a blood-based AD screen may be on the horizon (119–123).

TAU is most closely related to neuronal death and is hypothesized to be fragmented in the blood. For more accurate results, biotechnology companies have been developing novel methods and technologies, with more overall sensitivity for biomolecules detection that could be used for future biomarker discoveries. Henriksen and colleagues described the recent development of a digital ELISA for total TAU in serum and suggest that this type of technology may also enable the detection of Aβ peptides (124). TAU levels in peripheral bodily fluids need more research for one to understand how the increased brain levels of TAU in AD might be reflected in elevated levels of TAU in blood.

6. Conclusion

6. Conclusion

There is an urgent need for a simple screening procedure that can identify patients with AD in a differential, inexpensive and non-invasive manner. The identification of novel and valid biomarkers in the peripheral fluids such as blood and CSF is highly desirable and can become an essential tool for diagnosing Alzheimer's disease.

The work here describes the TAU Thr231 phosphorylation potential as a biomarker for AD, but also its function and its contribution to TAU localization in SH-SY5Y neuroblastoma cells

The experimental data revealed that cellular differentiation induced by treatment with RA increased expression of TAU phosphorylated at Thr231. In undifferentiated SH-SY5Y cells, pTAU231 was located mainly in the nucleus and, in contrast, TAU and pTAU231 were redistributed in the neurites and in the soma of SH-SY5Y cells induced to differentiate by retinoic acid (RA). This appears to suggest that the phosphorylation of the Thr231 residue may be a relevant process in cell differentiation.

As a CSF biomarker, the ratio of pTAU231/TAU levels discriminated significantly the AD group for the non-AD group. Moreover, TAUpThr231/t-TAU ratio levels improved diagnostic accuracy when compared with the mostly used pTAU181/t-TAU ratio levels in patients with AD.

These findings indicate that pTAU231/t-TAU ratio levels may be a valuable marker for the clinical diagnosis of AD, irrespective of age and gender.

7. References

7. References

1. Prince M, Comas-Herrera A, Knapp M, Guerchet M, Karagiannidou M. World Alzheimer Report 2016: Improving healthcare for people living with dementia. Alzheimer's Dis Int. 2016;

2. Jellinger KA. Alzheimer 100 – highlights in the history of Alzheimer research. J Neural Transm. 2006;113:1603–23.

3. Hippius H, Neundörfer G. The discovery of Alzheimer's disease. Dialogues Clin Neurosc. 2003;5(1):101–8.

4. Alzheimer A. No Über eine eigenartige Erkrankung der Hirnrinde. Allg Z Psychiatry Psych-Gerichtl Med. 1907;64:146–8.

5. Stelzma RA, Schnitzlein HN, Murllagh FR. An English Translation of Alzheimer's 1907 Paper, "Uber eine eigenartige Erkankung der Hirnrinde." Clin Anat. 1995;8:429–31.

6. Ballard C, Gauthier S, Corbett A, Brayne C, Aarsland D, Jones E. Alzheimer's disease. Lancet [Internet]. Elsevier Ltd; 2011;377(9770):1019–31. Available from: http://dx.doi.org/10.1016/S0140-6736(10)61349-9

7. Braak H, Braak E. Neuropathological stageing of Alzheimer-related changes. Acta Neuropathol. 1991;82:239–59.

8. Association A. 2017 Alzheimer's Disease Facts and Figures. Alzheimers Dement. 2017;13:325–73.

9. Braak H, Braak E. Morphological Criteria for the Recognition of Alzheimer's Disease and the Distribution Pattern of Cortical Changes Related to This Disorder. Neurobiol Aging. 1994;15(3):355–6.

10. Fox NC, Warrington EK, Freeborough PA, Hartikainen P, Kennedy AM, Stevens JM, et al. Presymptomatic hippocampal atrophy in Alzheimer's disease. A longitudinal MRI study. Brain [Internet]. 1996;119(6):2001–7. Available from: http://ovidsp.ovid.com/ovidweb.cgi?T=JS&PAGE=reference&D=med4&NEWS=N&AN=9010004\nhttp://ovidsp.ovid.com/ovidweb.cgi?T=JS&PAGE=reference&D=emed4&NEWS=N&AN=1997022963

11. Thal DR, Rub U, Orantes M, Braak H. Phases of Aβ-deposition in the human brain and its relevance for the development of AD. Neurology [Internet]. 2002;58(12):1791–800. Available from: http://www.neurology.org/cgi/doi/10.1212/WNL.58.12.1791

12. Delacourte A. The natural and molecular history of Alzheimer's disease. J Alzheimers Dis. 2006;9(3 Suppl):187–94.

13. Castellani RJ, Rolston RK, Smith MA. Alzheimer Disease. Disease-a-Month. 2011;56(9):1–60.

14. Selkoe DJ, Schenk D. Alzheimer's disease: molecular understanding predicts amyloid-based therapeutics. Annu Rev Pharmacol Toxicol [Internet]. 2003;43(1):545–84. Available from: http://www.annualreviews.org/doi/abs/10.1146/annurev.pharmtox.43.100901.140248\nhttp://www.ncbi.nlm.nih.gov/pubmed/12415125

15. Zheng H, Koo EH. The amyloid precursor protein: beyond amyloid. Mol Neurodegener. 2006;1(5):1–12.

16. Canter RG, Penney J, Tsai L-H. The road to restoring neural circuits for the treatment of Alzheimer's disease. Nature [Internet]. 2016;539(7628):187–96. Available from: http://www.nature.com/doifinder/10.1038/nature20412

17. Mucke L, Selkoe DJ. Synaptic and Network Dysfunction. Cold Spring Harb Perspect Med. 2012;1–17.

18. Hardy J, Selkoe DJ. The amyloid hypothesis of Alzheimer's disease: progress and problems on the road to therapeutics. Science [Internet]. 2002;297(5580):353–6. Available from: http://www.ncbi.nlm.nih.gov/pubmed/12130773

19. Serrano-Pozo A, Frosch MP, Masliah E, Hyman BT. Neuropathological alterations in Alzheimer disease. Cold Spring Harb Perspect Med. 2011;1(1):1–23.

20. Rosa IM, Henriques AG, Carvalho L, Oliveira J, Da Cruz E Silva O a. B. Screening Younger Individuals in a Primary Care Setting Flags Putative Dementia Cases and Correlates Gastrointestinal Diseases with Poor Cognitive Performance. Dement Geriatr Cogn Disord. 2017;43(1-2):15–28.

21. Carlsson CM. Type 2 diabetes mellitus, dyslipidemia, and Alzheimer's disease. J Alzheimers Dis [Internet]. 2010;20(3):711–22. Available from: http://www.pubmedcentral.nih.gov/articlerender.fcgi?artid=4235787&tool=pmcentrez&rendertype=abstract

22. Sennvik K, Fastbom J, Blomberg M, Wahlund L, Winblad B, Benedikz E. Levels of alfa- and beta -secretase cleaved amyloid precursor protein in the cerebrospinal fuid of Alzheimer's disease patients. Neurosci Lett. 2000;278:169–72.

23. Heaad E, Powell D, Gold BT, Schmitt FA. Alzheimer's Disease in Down Syndrome. Eur J Neurodegener Dis. 2012;1(3):353–64.

24. Duff K, Eckman C, Zehr C, Yu X, Prada CM, Perez-tur J, et al. Increased Amyloid-β42(43) in Brains of Mice Expressing Mutant Presenilin 1. Nature. 1996. p. 710–3.

25. Liu C-C, Liu C-C, Kanekiyo T, Xu H, Bu G. Apolipoprotein E and Alzheimer disease: risk, mechanisms and therapy. Nat Rev Neurol [Internet]. Nature Publishing Group; 2013;9(2):106–18. Available from: http://dx.doi.org/10.1038/nrneurol.2012.263

26. Lambert JC, Amouyel P. Genetics of Alzheimer's disease: New evidences for an old hypothesis? Curr Opin Genet Dev [Internet]. Elsevier Ltd; 2011;21(3):295–301. Available from: http://dx.doi.org/10.1016/j.gde.2011.02.002

27. Michaelson DM. APOE ε4: The most prevalent yet understudied risk factor for Alzheimer's disease. Alzheimer's Dement. 2014;10(6):861–8.

28. Greenberg DS, Sunada Y, Campbell KP, Yaffe D, Nudel U. Protective effect of apolipoprotein E type 2 allele for late onset Alzheimer disease. Nature [Internet]. 1994;8(4):340–4. Available from: papers2://publication/doi/10.1038/ng1294-340

29. Farrer LA, Cupples AL, Kukull W a, Mayeux R, Myers RH, Pericak-vance M a, et al. Effects of Age , Sex , and Ethnicity on the Association Between Apolipoprotein E Genotype and Alzheimer Disease. JAMA J Am Med Assoc [Internet]. 1997;278:1349–56. Available from: http://jama.ama-assn.org/content/278/16/1349%5Cnhttp://jama.ama-assn.org/content/278/16/1349.full.pdf%5Cnhttp://jama.ama-assn.org/content/278/16/1349.short

30. Harold D, Abraham R, Hollingworth P, Sims R, Hamshere M, Pahwa JS, et al. Genome-Wide Association Study Identifies Variants at CLU and PICALM Associated with Alzheimer's Disease, and Shows Evidence for Additional Susceptibility Genes. Nat Genet. 2009;41(10):1088–93.

31. Hollingworth P, Harold D, Sims R, Gerrish A, Lambert J-C, Carrasquillo MM, et al. Common variants at ABCA7, MS4A6A/MS4A4E, EPHA1, CD33 and CD2AP are associated with Alzheimer's disease. Nat Genet [Internet]. 2011;43(5):429–35. Available from: http://www.pubmedcentral.nih.gov/articlerender.fcgi?artid=3084173&tool=pmcentrez&rendertype=abstract

32. Kamboh MI, Demirci FY, Wang X, Minster RL, Carrasquillo MM, Pankratz VS, et al. Genome-wide association study of Alzheimer's disease. Transl Psychiatry. 2012;2(April):1–7.

33. Lausted C, Lee I, Zhou Y, Qin S, Sung J, Price ND, et al. Systems approach to neurodegenerative disease biomarker discovery. Annu Rev Pharmacol Toxicol [Internet]. 2014;54(October):457–81. Available from: http://www.ncbi.nlm.nih.gov/pubmed/24160693

34. Nordberg A, Rinne JO, Kadir A, Långström B. The use of PET in Alzheimer disease. Nat Rev Neurol [Internet]. Nature Publishing Group; 2010;6(2):78–87. Available from: http://www.ncbi.nlm.nih.gov/pubmed/20139997

35. Thakur S, Rao SN. The Handbook of Biomarkers. Igarss 2014. 2014. 1-5 p.

36. Lewczuk P, Riederer P, O'Bryant SE, Verbeek MM, Dubois B, Visser PJ, et al. Cerebrospinal fluid and blood biomarkers for neurodegenerative dementias: An update of the Consensus of the Task Force on Biological Markers in Psychiatry of the World Federation of Societies of Biological Psychiatry. World J Biol Psychiatry [Internet]. 2017;(October):1–85. Available from: https://www.tandfonline.com/doi/full/10.1080/15622975.2017.1375556

37. Anoop A, Singh PK, Jacob RS, Maji SK. CSF Biomarkers for Alzheimer ' s Disease Diagnosis. Int J Alzheimer's Dis. 2010;1–12.

38. Bradley T. Hyman, Creighton H. Phelps, Thomas G. Beach, Eileen H. Bigio, Nigel J. Cairns, Maria C. Carrillo, Dennis W. Dickson, Charles Duyckaerts, Matthew P. Frosch, Eliezer Masliah, Suzanne S. Mirra, Peter T. Nelson, Julie A. Schneider, Dietmar Rudolf T and TJM. National Institute on Aging–Alzheimer's Association guidelines for the neuropathologic assessment of Alzheimer's disease. Alzheimers Dement. 2012;8(1):1–13.

39. Klafki H-W, Staufenbiel M, Kornhuber J, Wiltfang J. Therapeutic approaches to Alzheimer's disease. Brain [Internet]. 2006;129(11):2840–55. Available from: https://academic.oup.com/brain/article-lookup/doi/10.1093/brain/awl280

40. Atkinson A.J. J, Colburn WA, DeGruttola VG, DeMets DL, Downing GJ, Hoth DF, et al. Biomarkers and surrogate endpoints: Preferred definitions and conceptual framework. Clin Pharmacol Ther. 2001;69(3):89–95.

41. Consensus report of the Working Group on: molecular and biochemical markers of Alzheimer's disease. Neurobiol Aging. 1998;19(2):109–16.

42. Hampel H, Frank R, Broich K, Teipel SJ, Katz RG, Hardy J, et al. Biomarkers for Alzheimer's disease: academic, industry and regulatory perspectives. Nat Rev Drug Discov [Internet]. Nature Publishing Group; 2010;9(7):560–74. Available from: http://www.nature.com/doifinder/10.1038/nrd3115

43. Blennow HK, Zetterberg), Blennow K, Blennow K, Hampel H, Weiner M, et al. Cerebrospinal fluid and plasma biomarkers in Alzheimer disease. Nat Publ Gr [Internet]. Nature Publishing Group; 2010;6(16104):131–44. Available from: http://dx.doi.org/10.1038/nrneurol.2010.4

44. Lewczuk P, Kornhuber J. Neurochemical dementia diagnostics in Alzheimer's disease: where are we now and where are we going? Expert Rev Proteomics [Internet]. 2011;8(4):447–58. Available from: http://www.tandfonline.com/doi/full/10.1586/epr.11.37

45. Hulstaert F, Blennow K, Ivanoiu a, Schoonderwaldt HC, Riemenschneider M, De Deyn PP, et al. Improved discrimination of AD patients using beta-amyloid(1-42) and tau levels in CSF. Neurology [Internet]. 1999;52(8):1555–62. Available from: http://www.ncbi.nlm.nih.gov/pubmed/10331678

46. Wiltfang J, Esselmann H, Bibl M, Hüll M, Hampel H, Kessler H, et al. Amyloid β peptide ratio 42/40 but not Aβ42 correlates with phospho-Tau in patients with low- and high-CSF Aβ40 load. J Neurochem. 2007;101(4):1053–9.

47. Hampel H, Blennow K, Shaw LM, Hoessler YC, Trojanowski JQ. Total and Phosphorylated Tau Protein as Biological Markers of Alzheimer's Disease. Exp Gerontol. 2010;45(1):1–21.

48. Vandermeeren M, Mercken M, Vanmechelen E, Six J, Voorde A Van De, Martin J, et al. Detection of Tau Proteins in Normal and Alzheimer's Disease Cerebrospinal Fluid with a Sensitive Sandwich Enzyme-Linked Immunosorbent Assay. J Neurochem. 1993;1828–34.

49. Zetterberg H, Wahlund LO, Blennow K. Cerebrospinal fluid markers for prediction of Alzheimer's disease. Neurosci Lett. 2003;352(1):67–9.

50. Humpel C. Identifying and validating biomarkers for Alzheimer's disease [Internet]. Trends in Biotechnology. 2011 [cited 2016 Jun 16]. p. 26–32. Available from: http://www.ncbi.nlm.nih.gov/pubmed/20971518

51. Lewczuk P, Zimmermann R, Wiltfang J, Kornhuber J. Neurochemical dementia diagnostics: A simple algorithm for interpretation of the CSF biomarkers. J Neural Transm. 2009;116(9):1163–7.

52. Drubin DG, Kirschner MW. Tau Protein Function in Living Cells. J Cell Biol. 1986;103(6):2739–46.

53. Schraen- S. Tau as a biomarker of neurodegenerative diseases. Biomarkers Med. 2008;2(Ld):363–84.

54. Buée L, Bussiere T, Buée-Scherrer V, Delacourte A, Hof PR. Tau protein isoforms , phosphorylation and role in neurodegenerative. Brain Res Rev. 2000;33:95–130.

55. Coedert M, Spillantini MC, Rutherford D, Crowther RA. Multiple lsoforms of Human Microtubule-Associated Protein Tau : Sequences and localization in Neurofibrillah Tangles of Alzheimer ' s Disease is found. Neuron. 1989;3:519–26.

56. Martin L, Latypova X, Terro F. Post-translational modifications of tau protein : Implications for Alzheimer's disease. Neurochem Int [Internet]. Elsevier Ltd; 2011;58(4):458–71. Available from: http://dx.doi.org/10.1016/j.neuint.2010.12.023

57. Planel E, Sun X, Takashima A. Role of GSK-3 b in Alzheimer's Disease Pathology. Drug Dev Res. 2002;56:491–510.

58. Gendron TF, Petrucelli L. The role of tau in neurodegeneration. Mol Degener. 2009;4(13).

59. Shahani N, Brandt R. Functions and malfunctions of the tau proteins. Cell Mol Life Sci. 2002;59(10):1668–80.

60. Wang J, Liu F. Microtubule-associated protein tau in development , degeneration and protection of neurons. Prog Neurobiol. 2008;85:148–75.

61. Avila J, Lucas JJ, Perez M, Hernandez F. Role of tau protein in both physiological and pathological conditions. Physiol Rev. 2004;84(2):361–84.

62. Hanger DP, Anderton BH, Noble W. Tau phosphorylation : the therapeutic challenge for neurodegenerative disease. Trends Mol Med. 2009;15(3):112–9.

63. Hanger DP, Byers HL, Leung K, Saxton MJ, Seereeram A, Reynolds CH, et al. Novel Phosphorylation Sites in Tau from Alzheimer Brain Support a Role for Casein Kinase 1 in Disease Pathogenesis. J Biol Chem. 2007;282(32):23645–54.

64. Oliveira J, Costa M, de Almeida MSC, da Cruz e Silva OAB, Henriques AG. Protein Phosphorylation is a Key Mechanism in Alzheimer's Disease. J Alzheimer's Dis [Internet]. 2017;1–26. Available from: http://www.medra.org/servlet/aliasResolver?alias=iospress&doi=10.3233/JAD-170176

65. Biernat J, Gustke N, Drewes G, Mandelkow E, Mandelkow E. Phosphorylation of Ser262 strongly reduces binding of tau to microtubules: Distinction between PHF-like immunoreactivity and microtubule binding. Neuron. 1993;11(1):153–63.

66. Cho J-H, Johnson GVW. Primed phosphorylation of tau at Thr231 by glycogen synthase kinase 3beta (GSK3beta) plays a critical role in regulating tau's ability to bind and stabilize microtubules. J Neurochem. 2004;88(2):349–58.

67. Lu PJ, Wulf G, Zhou XZ, Davies P, Lu KP. The prolyl isomerase Pin1 restores the function of Alzheimer-associated phosphorylated tau protein. Nature [Internet]. 1999;399(6738):784–8. Available from: http://dx.doi.org/10.1038/21650

68. Sergeant N, Bue L. Tau protein as a differential biomarker of tauopathies. Biochim Biophys Acta. 2005;1739:179–97.

69. Ferrer I, Puig B, Freixes M, Ribé E, Dalfó E, Avila J. Current Advances on Different Kinases Involved in Tau Phosphorylation , and Implications in Alzheimer ' s Disease and Tauopathies. Curr Alzheimer Res. 2005;2:3–18.

70. Takashima A. GSK-3 is essential in the pathogenesis of Alzheimer ' s disease. J Alzheimer's Dis. 2006;9:309–17.

71. http://cnr.iop.kcl.ac.uk/hangerlab/tautable.

72. Liu F, Grundke-iqbal I, Iqbal K, Gong C. Contributions of protein phosphatases PP1 , PP2A , PP2B and PP5 to the regulation of tau phosphorylation. Eur J Neurosci. 2005;22:1942–50.

73. Wang J, Gong C-X, Zaidi T, Grundke-Iqbal I, Iqbal K. Dephosphorylation of Alzheimer Paired Helical Filaments by Protein Phosphatase-2A and -2B. J Biol Chem. 1995;270(9):4854–60.

74. Mawal-Dewan M, Henley J, Van De Voorde A, Trojanowski JQ, Lee VMY. The phosphorylation state of tau in the developing rat brain is regulated by phosphoprotein phosphatases. J Biol Chem. 1994;269(49):30981–7.

75. Terwel D, Dewachter I, Van Leuven F. Axonal transport, tau protein, and neurodegeneration in Alzheimer's disease. Neuromolecular Med [Internet]. 2002;2(2):151–65. Available from: http://www.ncbi.nlm.nih.gov/pubmed/12428809

76. Hirokawa N, Funakoshi T, Sato-Harada R, Kanai Y. Selective stabilization of tau in axons and microtubule-associated protein 2C in cell bodies and dendrites contributes to polarized localization of cytoskeletal proteins in mature neurons. J Cell Biol. 1996;132(4):667–79.

77. Johnson G V, Stoothoff WH. Tau phosphorylation in neuronal cell function and dysfunction. J Cell Sci. 2004;117(Pt 24):5721–9.

78. Sergeant N, Bretteville A, Hamdane M, Grognet P, Bombois S, Blum D, et al. Biochemistry of Tau in Alzheimer's disease and related neurological disorders. Expert Rev Proteomics. 2008;5(2):207–24.

79. Iqbal K, Liu F, Gong C-X, Grundke-Iqbal I. Tau in Alzheimer Disease and Related Tauopathies. Curr Alzheimer Res. 2010;7(8):656–64.

80. Salehi A, Delcroix JD, Mobley WC. Traffic at the intersection of neurotrophic factor signaling and neurodegeneration. Trends Neurosci. 2003;26(2):73–80.

81. Friedhoff P, von Bergen M, Mandelkow E-M, Mandelkow E. Structure of tau protein and assembly into paired helical filaments. Biochim Biophys Acta - Mol Basis Dis [Internet]. 2000;1502(1):122–32. Available from: http://www.sciencedirect.com/science/article/pii/S0925443900000387

82. Dubois B, Feldman HH, Jacova C, Dekosky ST, Barberger-gateau P, Cummings J, et al. Research criteria for the diagnosis of Alzheimer ' s disease : revising the NINCDS – ADRDA criteria. Lancet Neurol. 2007;6:734–46.

83. Grundman M, Sencakova D, Jack CR, Petersen RC, Kim HT, Schultz A, et al. Brain MRI Hippocampal Volume and Prediction of Clinical Status in a Mild Cognitive Impairment Trial. J Mol Neurosci. 2002;19:23–7.

84. Decarli C. Mild cognitive impairment : prevalence , prognosis , aetiology , and treatment. Lancet Neurol. 2003;2:15–21.

85. Gauthier S, Reisberg B, Zaudig M, Petersen RC, Ritchie K, Broich K, et al. Mild cognitive impairment. Lancet. 2006;367:1262–70.

86. Bullock R. Mild cognitive impairment. Psychiatry. 2007;7(1):36–8.

87. Buerger K, Teipel SJ, Zinkowski R. CSF tau protein phosphorylated at threonine 231 correlates with cognitive decline in MCI subjects CSF tau protein phosphorylated at threonine 231 correlates with cognitive decline in. Neurology. 2012;59:627–9.

88. Blennow K, Vanmechelen E, Hampel H. CSF total tau, Abeta42 and phosphorylated tau protein as biomarkers for Alzheimer's disease. Mol Neurobiol [Internet]. 2001;24(1-3):87–97. Available from: http://www.ncbi.nlm.nih.gov/pubmed/11831556

89. Mitchell AJ. CSF phosphorylated tau in the diagnosis and prognosis of mild cognitive impairment and Alzheimer's disease: a meta-analysis of 51 studies. J Neurol Neurosurg Psychiatry [Internet]. 2009;80(9):966–75. Available from: http://jnnp.bmj.com/cgi/doi/10.1136/jnnp.2008.167791

90. Blom ES, Giedraitis V, Zetterberg H, Fukumoto H, Blennow K, Hyman BT, et al. Rapid progression from mild cognitive impairment to alzheimer's disease in subjects with elevated levels of tau in cerebrospinal fluid and the Apoe ε4/ε4 genotype. Dement Geriatr Cogn Disord. 2009;27(5):458–64.

91. Sämgård K, Zetterberg H, Blennow K, Hansson O, Minthon L, Londos E. Cerebrospinal fluid total tau as a marker of Alzheimer's disease intensity. Int J Geriatr Psychiatry. 2010;25(4):403–10.

92. Buerger K, Alafuzoff I, Ewers M, Pirttilä T, Zinkowski R, Hampel H. No correlation between CSF tau protein phosphorylated at threonine 181 with neocortical neurofibrillary pathology in Alzheimer's disease [2]. Brain. 2007;130(10):180–1.

93. Kohnken R, Buerger K, Zinkowski R, Miller C, Kerkman D, Debernardis J, et al. Detection of tau phosphorylated at threonine 231 in cerebrospinal fluid of Alzheimer's disease patients. Neurosci Lett. 2000;287(3):187–90.

94. Buerger K, Ewers M, Pirttilä T, Zinkowski R, Alafuzoff I, Teipel SJ, et al. CSF phosphorylated tau protein correlates with neocortical neurofibrillary pathology in Alzheimer's disease. Brain. 2006;129(11):3035–41.

95. Vincent I, Zheng JH, Dickson DW, Kress Y, Davies P. Mitotic phosphoepitopes precede paired helical filaments in Alzheimer's disease. Neurobiol Aging. 1998;19(4):287–96.

96. Kovalevich J, Langford D. Considerations for the Use of SH - SY5Y Neuroblastoma Cells in Neurobiology. Neuronal Cell Cult Methods Protoc Methods Mol Biol. 2013;1078:9–21.

97. Dwane S, Durack E, Kiely PA. Optimising parameters for the differentiation of SH-SY5Y cells to study cell adhesion and cell migration. BMC Res Notes [Internet]. BMC Research Notes; 2013;6(1):366. Available from: http://bmcresnotes.biomedcentral.com/articles/10.1186/1756-0500-6-366

98. F. da Rocha J. Understanding APP-dependent neuronal differentiation. University of Aveiro; 2011.

99. Henriques AG, Oliveira JM, Gomes B, Ruivo R, Da Cruz E Silva EF, Da Cruz E Silva OAB. Complexing Aβ prevents the cellular anomalies induced by the peptide alone. J Mol Neurosci. 2014;53(4):661–8.

100. W. Burry R. Immunocytochemistry, A Practical Guide for Biomedical Research. Springer New York Dordrecht Heidelberg London; 2010.

101. GE Healthcare Life Sciences. Western Blotting: Principles and Methods. 2014;176.

102. Andreasen N, Minthon L, Davidsson P, Vanmechelen E, Vanderstichele H, Winblad B, et al. Evaluation of CSF-tau and CSF-Aβ 42 as diagnostic markers for Alzheimer disease in clinical practice. Arch Neurol. 2001;58(3):373–9.

103. Marcusson J, Hallbeck M, Agholme L. An In Vitro Model for Neuroscience : Differentiation of SH-SY5Y Cells into Cells with Morphological and Biochemical Characteristics of Mature Neurons. J Alzheimer's Dis. 2010;20:1069–82.

104. Bulbarelli A, Lonati E, Cazzaniga E, Gregori M, Masserini M. Pin1 affects Tau phosphorylation in response to Aβ oligomers. Mol Cell Neurosci [Internet]. Elsevier Inc.; 2009;42(1):75–80. Available from: http://dx.doi.org/10.1016/j.mcn.2009.06.001

105. Oliveira JM, Henriques AG, Martins F, Rebelo S, Da Cruz E Silva O a B. Amyloid-β Modulates Both AβPP and Tau Phosphorylation. J Alzheimer's Dis. 2015;45(2):495–507.

106. Jämsä A, Hasslund K, Cowburn RF, Bäckström A, Vasänge M. The retinoic acid and brain-derived neurotrophic factor differentiated SH-SY5Y cell line as a model for Alzheimer's disease-like tau phosphorylation. Biochem Biophys Res Commun. 2004;319(3):993–1000.

107. Smith CJ, Anderton BH, Davis DR, Gallo JM. Tau isoform expression and phosphorylation state during differentiation of cultured neuronal cells. FEBS Lett. 1995;375(0014-5793):243–8.

108. Chen Q, Zhou Z, Zhang L, Xu S, Chen C, Yu Z. The Cellular Distribution and Ser262 Phosphorylation of Tau Protein Are Regulated by BDNF In Vitro. PLoS One. 2014;9(3):1–10.

109. Korzhevskii DE, Karpenko MN, Kirik O V. Microtubule-Associated Proteins as Indicators of Differentiation and the Functional State of Nerve Cells. Neurosci Behav Physiol. 2012;42(3):215–22.

110. Dotti CG, Banker G a., Binder LI. The expression and distribution of the microtubule-associated proteins tau and microtubule-associated protein 2 in hippocampal neurons in the rat in situ and in cell culture. Neuroscience. 1987;23(1):121–30.

111. Greenwood JA, Johnson GVW. Localization and in Situ Phosphorylation State of Nuclear Tau. Exp Cell Res. 1995;220:332–7.

112. Spiegel J, Pirraglia E, Osorio RS, Glodzik L, Li Y, Louis LA Saint, et al. Greater Specificity for Cerebrospinal Fluid P-tau231 over P- tau181 in the Differentiation of Healthy Controls from Alzheimer's Disease. J Alzheimer's Dis. 2015;49(1):93–100.

113. Seppälä TT, Nerg O, Koivisto AM, Rummukainen J, Puli L, Zetterberg H, et al. CSF biomarkers for Alzheimer disease correlate with cortical brain biopsy findings. Neurology. 2012;78(20):1568–75.

114. Blennow K, Wallin A, Agren H. Tau Protein in Cerebrospinal Fluid. A Biochemical Marker for Axonal Degeneration in Alzheimer Disease? Mol Chem Neuropathol. 1995;26(3):231–45.

115. Tapiola T, Alafuzoff I, Herukka S, Parkkinen L, Hartikainen P, Soininen H, et al. Cerebrospinal Fluid β-Amyloid 42 and Tau Proteins as Biomarkers of Alzheimer-Type Pathologic Changes in the Brain. Arch Neurol. 2009;66(3):382–9.

116. Ishiguro K, Ohno H, Arai H, Yamaguchi H. Phosphorylated tau in human cerebrospinal fuid is a diagnostic marker for Alzheimer's disease. Neurosci Lett. 1999;270:91–4.

117. Blennow K, Hampel H. Review CSF markers for incipient Alzheimer 's disease. Lancet Neurol. 2003;2(October):605–13.

118. Fattahi S, Kazemipour N, Valizadeh J, Hashemi M, Ghazizade H, Removal A. Comparison of Different Albumin Removal Methods for Evaluation of Human Serum Proteome. 2010;1–5.

119. Laske C, Leyhe T, Stransky E, Hoffmann N, Fallgatter AJ, Dietzsch J. Identification of a blood-based biomarker panel for classification of Alzheimer's disease. Int J Neuropsychopharmacol [Internet]. 2011;14(09):1147–55. Available from: https://academic.oup.com/ijnp/article-lookup/doi/10.1017/S1461145711000459

120. Laske C, Schmohl M, Leyhe T, Stransky E, Maetzler W, Berg D, et al. Immune profiling in blood identifies sTNF-R1 performing comparably well as biomarker panels for classification of alzheimer's disease patients. J Alzheimer's Dis. 2013;34(2):367–75.

121. O'Bryant SE, Xiao G, Barber R, Reisch J, Doody R, Fairchild T, et al. A serum protein-based algorithm for the detection of Alzheimer disease. Arch Neurol [Internet]. 2010;67(9):1077–81. Available from: http://www.ncbi.nlm.nih.gov/pubmed/20837851\nhttp://www.pubmedcentral.nih.gov/articlerender.fcgi?artid=PMC3069805

122. O'Bryant SE, Xiao G, Barber R, Huebinger R, Wilhelmsen K, Edwards M, et al. A blood-based screening tool for Alzheimer's disease that spans serum and plasma: Findings from TARC and ADNI. PLoS One. 2011;6(12).

123. Doecke JD. Blood-Based Protein Biomarkers for Diagnosis of Alzheimer Disease. Arch Neurol [Internet]. 2012;69(10):1318. Available from: http://archneur.jamanetwork.com/article.aspx?doi=10.1001/archneurol.2012.1282

124. Henriksen K, Wang Y, Sørensen MG, Barascuk N, Suhy J, Pedersen JT, et al. An Enzyme-Generated Fragment of Tau Measured in Serum Shows an Inverse Correlation to Cognitive Function. PLoS One. 2013;8(5).

8. Appendix

8. Appendix

I. Cell Culture Reagents and Equipment

Equipment

- Hera cell CO2 incubator (Heraeus)
- Safety cabinet Hera safe (Heraeus)
- Inverted optical microscope (LEICA)
- Hemacytometer (Sigma)
- Sonicator (U200S (IKA))
- Bath SBB6 (Grant)

Solutions

- SH-SY5Y Complete Medium (Eagle's Minimum Essential Medium/F12 Medium 1:1)

  - 4.805 g MEM
  - 5.315 g F12
  - 1.5 g NaHCO3
  - 0.055 g Sodium Pyruvate
  - 10 mL Streptomycin/Penicillin/Amphotericin solution
  - 100 mL 10% FBS
  - 2.5 mL L-glutamine (200 mM stock solution)

Dissolve in deionized H2O. Adjust the pH to 7.2-7.3. Adjust the volume to 1000 mL with deionized H2O.
For other combinations of FBS, replace 100 mL FBS with 10 mL (1% FBS MEM:F12) or remove FBS (serum-free MEM:F12).

- PBS (1x)

For a final volume of 500 ml, dissolve one pack of BupH Modified Dulbecco's Phosphate Buffered Saline Pack (Pierce) in deionised H2O. Final composition:

- 8 mM Sodium Phosphate
- 2 mM Potassium Phosphate
- 140 mM Sodium Chloride
- 10 mM Potassim Chloride

Sterilize by filtering through a 0.2 µm filter and store at 4oC.

- Trypsin-EDTA 0,05% (Thermo)

- Trypan Blue solution cell culture tested (Sigma)

- RIPA buffer

To 980 µL of RIPA buffer (Sigma-Aldrich) add:

- 20 µL Protease inhibitor cocktail (Roche)

- Beta-Amyloid 1-42, TFA (GenicBio)

II. Protein Content Determination

Equipment

- Tecan 5000

Reagents

- BCA assay kit (Pierce, Rockfort, IL)
- Bovine Serum Albumin (BSA) (Pierce)
- Working Reagent (WB) (50 Reagent A : 1 Reagent B)
    - Reagent A: sodium carbonate, sodium bicarbonate, BCA and sodium tartrate in 0,2N sodium hydroxide
    - Reagent B: 4% cupric sulfate

III. SDS-PAGE

Equipment

- Electrophoresis system (Hoefer SE600 vertical unit)
- Electrophoresis power supply EPS 1000 (Amersham Pharmacia Biotec)

Reagents

- Acrylamide: Bis-Acrylamide 29:1 solution 40%, Dnase, Rnase free (Fisher)

- 10% APS (ammonium persulfate)

In 10 ml of deionised H2O dissolve 1 g of APS. Note: prepare fresh before use.

- 10% SDS (sodium dodecilsulfate)

In 10 ml of deionised H2O dissolve 1 g of SDS.

- LGB (Lower gel buffer) (4x)

To 900 ml of deionised H2O add:
- 181.65 g Tris
- 4 g SDS

Mix until the solutes have dissolved. Adjust the pH to 8.9 and adjust the volume to 1L with deionised H2O.

- **UGB (Upper gel buffer) (5x)**

To 900 ml of deionised H2O add:

- 75.69 g Tris

Mix until the solute has dissolved. Adjust the pH to 6.8 and adjust the volume to 1 L with deionised H2O.

- **Loading Gel Buffer (4x)**

- 2.5 mL 1 M Tris solution (pH 6.8) (250 mM)
- 0.8 g SDS (8%)
- 4 ml Glicerol (40%)
- 2 ml Beta-Mercaptoetanol (2%)
- 1 mg Bromofenol blue (0.01%)

Adjust the volume to 10 ml with deionised H2O. Store in darkness at room temperature.

- **1 M Tris (pH 6.8)**

To 150 ml of deionised H2O add:

- 30.3 g Tris base

Adjust the pH to 6.8 and adjust the final volume to 250 ml.

- **10x Running Buffer**

- 30.3 g Tris (250 mM)
- 144.2 g Glycine (2.5 M)
- 10 g SDS (1%)

Dissolve in deionised H2O, adjust the pH to 8.3 and adjust the volume to 1 L.

- **Stacking (upper) and Resolving (lower) gel solution**

	Stacking Gel	Resolving Gel	
	3.5%	5%	20%
- H2O	13.83 ml	18.59 ml	7.34 ml
- 29:1 Bis-Acrylamide	1.75 ml	3.75 ml	15 ml
- LGB (4x)	-	7.5 ml	7.5 ml
- UGB (5x)	4.0 ml	-	-
- 10% APS	200 µL	150 µL	150 µL
- 10% SDS	200 µL	-	-
- TEMED	20 µL	15 µL	15 µL
	20 mL	60 mL	

IV. Western-Blotting Solutions and Equipment

Equipment

- Transphor Electrophoresis unit (Hofer TE 42)
- Electrophoresis power supply EPS 1000 (Amersham Pharmacie Biotec)

Reagents

- **1x Transfer Buffer**

  - 3.03 g Tris (25 mM)
  - 14.41 g Glycine (192 mM)

Mix until solutes dissolution. Adjust the pH to 8.3 with HCl and adjust the volume to 800 ml with deionised H2O. Just prior to use add 200 ml of methanol (20%).

V. ImmunoBlotting Solutions

Equipment

- ChemiDoc Touch Imageing System (BioRad)

Reagents

- **10x TBS (Tris buffered saline)**

  - 12.11 g Tris (10 mM)
  - 87.66 g NaCl (150 mM)

Adjust the pH to 8.0 with HCl and adjust the volume to 1L with deionised H2O.

- **10x TBS-T (TBS+Tween)**

  - 12.11 g Tris (10 mM)
  - 87.66 g NaCl (150 mM)
  - 5 ml Tween20 (0.05%)

Adjust the pH to 8.0 with HCl and adjust the volume to 1L with deionised H2O.

- **Blocking solution**

5% of nonfat dried milk or BSA (Bovine Serum Albumine, Sigma) in 1x TBS-T.

- **Amersham ECL Select Western Blotting Detection Reagent (GE Healthcare Life Sciences)**

- **Membranes Stripping Solution** (500 ml)

  - 3.76 g Tris-HCl (pH 6.7) (62.5 mM)
  - 10 g SDS (2%)
  - 3.5 ml Beta-mercaptoetanol (100 mM)

Dissolve Tris and SDS in deionised H2O and adjust with HCl to pH 6.7. Add the mercaptoethanol and adjust volume to 500 ml.

VI. Immunoprecipitation

- Dynabeads® Protein G (Thermo Science)

- Blocking solution

Add 0.6g of BSA (Bovine Serum Albumine, Sigma) to 20 mL of PBS 1x.

VII. Imunocitochemistry

- Blocking solution

5% BSA (Bovine Serum Albumine, Sigma) in 1x PBS.

- Permeabilization solution

0.2% Triton X-100 Surfactant (Calbiochem) in 1x PBS.

- Fixing solution

4% PFA (Paraformaldheyde, Sigma) in 1x PBS

VIII. ELISA

- Human TAU [pT231] PhosphoELISA™ Kit, Invitrogen
- INNOTEST PHOSPHO-TAU [181P] Antigen, Innogenetics
- INNOTEST hTAU-Ag, Innogenetics
- INNOTEST β-amyloid [1-42], Innogenetics

IX. Albumin/IgG depletion

- ProteoSeek columns (IgG removal kit, Thermo Science)